Czech Technical University
in Prague
Faculty of Electrical Engineering

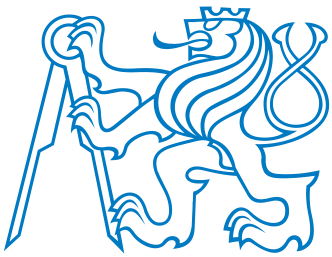

System for Measurement of Hemodynamic Parameters

Master's thesis

Department of Cybernetics

Author: Bc. Dominik Šídlo

Supervisor: Ing. Vratislav Fabián, Ph.D.

Prague, August 2020

MASTER'S THESIS ASSIGNMENT

I. Personal and study details

Student's name: **Šídlo Dominik** Personal ID number: **434818**

Faculty / Institute: **Faculty of Electrical Engineering**

Department / Institute: **Department of Cybernetics**

Study program: **Medical Electronics and Bioinformatics**

Specialisation: **Medical Instrumentation**

II. Master's thesis details

Master's thesis title in English:

System for Measurement of Hemodynamic Parameters

Master's thesis title in Czech:

Systém pro měření hemodynamických parametrů

Guidelines:

1) Perform a research on algorithms for pulse waveform analysis to determinate hemodynamic parameters of the cardiovascular system.
2) Get acquainted with the Python programming language and the Raspberry Pi platform.
3) Devise and implement algorithms for pulse waveform analysis particularly on determination of blood pressure and pulse wave velocity.
4) Devise and realize a connection between the existing pneumatic system and Raspberry Pi platform.
5) Perform measurements on a group of students and test the functionality of the proposed solution.
6) Prepare a technical documentation for the proposed solution.

Bibliography / sources:

[1] J. Unpingco, Python for Signal Processing. Cham: Springer International Publishing, 2014.
[2] P. Salvi, Pulse waves: how vascular hemodynamics affects blood pressure. Milan: Springer, 2012.
[3] G. Pedrizzetti a K. Perktold, Ed., Cardiovascular fluid mechanics: lectures held at CISM during July 2002. Wien: Springer, 2003.

Name and workplace of master's thesis supervisor:

Ing. Vratislav Fabián, Ph.D., Department of Physics, FEE

Name and workplace of second master's thesis supervisor or consultant:

Date of master's thesis assignment: **09.01.2020** Deadline for master's thesis submission: **14.08.2020**

Assignment valid until: **30.09.2021**

Ing. Vratislav Fabián, Ph.D.	doc. Ing. Tomáš Svoboda, Ph.D.	prof. Mgr. Petr Páta, Ph.D.
Supervisor's signature	Head of department's signature	Dean's signature

III. Assignment receipt

The student acknowledges that the master's thesis is an individual work. The student must produce his thesis without the assistance of others, with the exception of provided consultations. Within the master's thesis, the author must state the names of consultants and include a list of references.

.	
Date of assignment receipt	Student's signature

Author declaration

I declare that the presented work was developed independently and that I have listed all sources of information used within it in accordance with the methodical instructions for observing the ethical principles in the preparation of university theses.

Prague, the ....

Author signature

Acknowledgment

I would first like to thank my thesis advisor Ing. Vratislav Fabián, Ph.D. and Ing. Lukáš Matera. The door to their office was always open whenever I ran into trouble or had a question about my work, research or writing. I would also like to thank the participants who were involved in the validation measurement for this work. Without their passionate participation, the validation measurement could not have been successfully conducted.

Abstract

This master's thesis aims to design and implement a non-invasive system for the measurement of hemodynamic parameters. The system is based on the Raspberry Pi microcomputer, which controls a pneumatic system and acquires data. Further, the system is based on open-sourced platforms and doesn't require any licensed product. The data is evaluated in the Python programming language directly on the device. The system inflates a cuff placed on the arm over the brachial artery to suprasystolic pressure and captures pressure pulse waveforms through a differential sensor to a static pressure reference. From the pressure pulse waveform, the pulse wave velocity and the heart rate is computed through a script. During the inflation of the cuff, oscillometric pressure measurement is performed. The system is controlled through a touchscreen. Six students aged 20 to 24 years were tested on the system.

Keywords

Blood pressure, Oscillometric pulsations, Suprasystolic pressure, Pulse wave velocity (PWV), Raspberry Pi, Python

Abstrakt

Diplomová práce se zabývá návrhem a realizací systému pro neinvazivní měření hemodynamických parametrů. Systém je založen na mikropočítači Raspberry Pi, který ovládá pneumatický systém a snímá data. Dále je systém zcela založen na open source platformách a nevyžaduje žádný licencovaný produkt. Data jsou vyhodnocena v programovacím jazyce Python přímo na zařízení. Systém nafoukne manžetu umístěnou na paži nad brachiální tepnou na suprasystolický tlak a snímá vůči referenčnímu statickému tlaku pomocí diferenciálního senzoru tlakové pulzace. Z těch je následně pomocí skriptu vypočtena rychlost šíření pulzní vlny a srdeční tep. Během nafukování manžety je provedeno oscilometrické měření krevního tlaku. Ovládání systému je umožněno přes dotykový displej. Systém byl testován na skupině šesti studentů ve věku 20 až 24 let.

Klíčová slova

Krevní tlak, Oscilometrické pulzace, Suprasystolický tlak, Rychlost šíření pulzní vlny (PWV), Raspberry Pi, Python

Contents

List of Figures

List of Tables

List of abbreviations:

CVD Cardiovascular disease

PWV Pulse wave velocity

RPi Raspberry Pi

GUI Graphical user interface

SBP Systolic blood pressure

DBP Diastolic blood pressure

MAP Mean arterial pressure

ASI Arterial stiffness index

CO Cardiac output

HR Heart rate

SV Stroke volume

SVR Systemic vascular resistance

PP Pulse pressure

PPG Photoplethysmograph

PiCCO Pulse index continuous cardiac output

AIx Augmentation index

AP Augmented pressure

FF Form Factor

PPA Pulse pressure amplification

SEVR Subendocardial viability ratio

GPIO General-purpose input/output

RAM Random access memory

HDMI High-definition multimedia interface

USB Universal serial bus

DC Direct currenr

OS operating system

PWM Pulse wave modulation

SPI Serial peripheral interface

I2C Inter-integrated circuit

SPI Serial peripheral interface

ADC Analogue to digital converter

PCB Printed circuit board

LP Low-pass

HP High-pass

BHS The British Hypertension Society

1 Introduction

Cardiovascular diseases (CVDs) are rated as the number one cause of death today. In numbers, this means that about 31 % of deaths were caused by CVDs in past four years [1]. Researching further 85 % of CVDs are caused by atherosclerosis (clogging up of blood vessel) which is subjected to an abnormal build-up of fatty substances, thrombi, cholesterol and other plaques. The main diseases with fatal causes are ischaemic heart disease (heart attack) and cerebrovascular disease (stroke). A great focus is given to early on detection and prevention of these diseases through indices like hemodynamic parameters, glucose and lipids levels as well as overweight and obesity [2].

In this thesis, we were focusing on building a system that is capable of non-invasively assessing hemodynamic parameters, namely blood pressure, pulse wave velocity (PWV) and heart rate. Since PWV can be acquired through expensive systems used by medical professionals, we had to build a cheap system easy to use at home, that would mention parameters. The concept of this system has been based on the measurement of the blood pressure waveform with a single cuff with suprasystolic pressure pulsation measurement resembling a commonly used digital monitor for blood pressure measurement.

First hemodynamic parameters and the methods and algorithms for acquiring them were researched. We have decided that we will focus on the PWV, blood pressure and heart rate, although our system should be capable of assessing many more parameters.

Also, We have researched the tools we were using in our system. For the hardware part, the Raspberry Pi (RPi) platform was being used to control the pneumatic system and interpret the measured data. For the software, we were using the open-source programming language Python with all the tools it offers to create the analysing algorithms, controlling scripts, data acquisition scripts and to create a graphical user interface (GUI) for the control. To this part, we created technical documentation of all the components and described all the written scripts used.

The final system was being tested, on a group of students to validate the measurements. The system was supposed to be, non-invasive, accurate and portable to be used as a mean of personal healthcare.

2 Hemodynamic parameters

Hemodynamic parameters are parameters connected to the blood flow in the circulatory system of the human body. Good blood flow in the human body is key for the proper function of organs and the whole body. Many parameters have a great influence on it. From the consistency of the blood through all the channels that it flows and the function and shape of the main pump in our body, the heart, all have important parameters through which we can assess if the circulatory system is in proper shape or if there is a risk of CVDs. In this section, we have researched and determined the hemodynamic parameters that we wanted to measure and were interested in.

2.1 Blood pressure

A very important parameter connected to CVDs is blood pressure, although this term involves a few more parameters. It is important to notice that blood pressure depends on many factors. The age of the subject, the state of the arterial tree, the momentary conditions and digestion of substances influencing the circulatory system. They all have a great impact on the components of blood pressure (figure 1) and the current blood pressure levels. Also, the levels are dependent on the location of measurement [3].

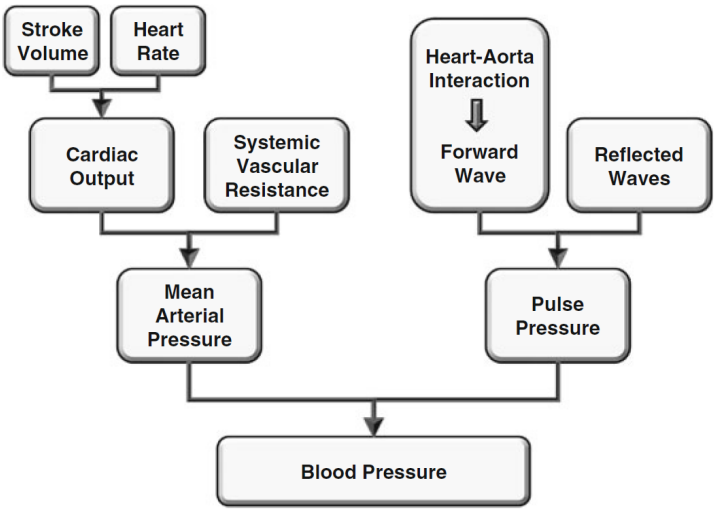

Figure 1: Components of blood pressure [4]

We will usually see a continuous blood pressure waveform. In this waveform, we can easily identify two main spots. Systolic blood pressure (SBP), which is the highest point of the waveform and resembles the outburst of blood from the hearts left ventricle. Diastolic blood pressure(DBP), which is the lowest level of the waveform and resembles the filling of the left ventricle. Further, the mean arterial pressure (MAP), which is the mean pressure in one period of the waveform can be computed. From the difference between SBP and DBP, we get the pulse pressure. Sometimes we can spot the dicrotic notch which is caused by the closing of the aortic flaps [5]. In the next sections, we will discuss these parameters on their own.

2.1.1 Blood pressure measurement

To measure blood pressure several methods can be used. In very serious cases the blood pressure monitoring is done directly with an invasive method. A catheter is introduced into the arteries and the pressure waveform is being directly traced with a pressure sensor placed on the end of the catheter or the pressure is transferred through a physiological saline solution in the catheter to a sensor outside. A very common and non-invasive way for blood pressure measurement is with a cuff on the brachial artery. There are many ways of assessing the blood pressure levels such as the auscultatory method and the oscillometric method. Both methods depend on sensing the internal pressure in the cuff which can be done with an electric sensor, mercury column or aneroid gauge. The auscultatory method determines the different pressure levels by listening to the Korotkoff sounds. This is usually done by a medical professional with a stethoscope or a microphone with an electronically evaluating system. The oscillometric method senses the small oscillations caused by the pulse waveform oscillating on the cuff strangled brachial artery with different intensities at different blood pressure levels. These methods work with the change in pressure of the slowly deflating cuff and are not used for continuous blood pressure measurement[6]. There are several novel methods of blood pressure measurement using an inflatable measuring cuff, impedance rheography, ultrasound or photoplethysmography [7] which we won't further explore in the detail.

2.1.2 Mean arterial pressure

As said before, Mean arterial pressure is the mean pressure in one period of the waveform (equation 1).

$$MAP = \frac{1}{T}\int_{t}^{t+T} p(t)dt \qquad \text{[mmHg]} \tag{1}$$

Another way to view mean arterial pressure is by simplifying the cardiovascular system, we can look at it as a simple hydraulic system resembling an electrical circuit. We have a source of pressure gradient and blood flow, namely the heart, the arterioles resembling the resistance and the conduit arteries resembling the connections. Cardiac output (CO), consisting of stroke volume (SV) and heart rate (HR), is resembling the current. Systemic vascular resistance (SVR) resembles resistance. And the pressure between the two extreme points resembles mean arterial pressure. Similarly, to Ohm's law we get a simple equation (equation 2)[4].

$$MAP = CO \cdot SVR \qquad \text{[mmHg]} \tag{2}$$

It is important to notice that the MAP remains in the arterial tree stable, unlike the pulse pressure. This means that the MAP will be very similar in the artery as in the peripheries. The value of MAP for CVD diagnosis is arguable. Although a high MAP is already a sign of overall high pressure, a patient with high values of pulse pressure, meaning having a true isolated systolic hypertension, can have the same MAP as a patient with pulse pressure in the normal range, therefore the MAP is not sufficiently covering the prediction of CVDs [4] and the three parameters stroke volume, heart rate and systemic vascular resistance are not sufficient predictors.

2.1.3 Pulse pressure

When measuring blood pressure, the main parameters shown are the SBP and DBP, these two points are the points to which the MAP fluctuates and the scale of this fluctuation is called pulse pressure (PP). This pressure fluctuation originates from the interaction between left ventricular ejection and the mechanical properties of the large

arteries (the forward wave) (figure 2). A great effect on the form of the waveform and PP have the reflected waves in the arterial tree [8].

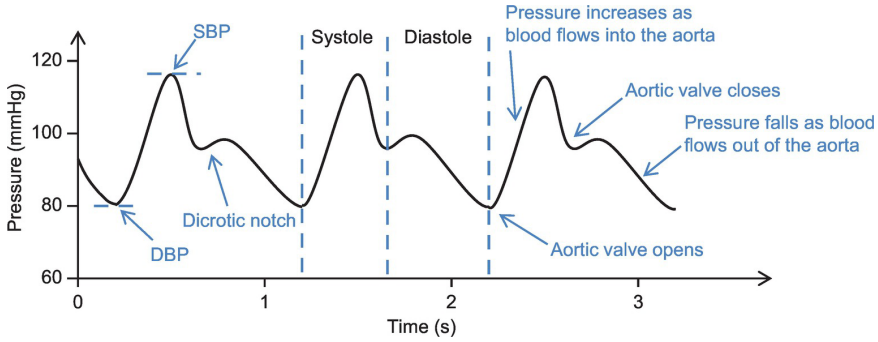

Figure 2: Systolic and diastolic blood pressure in the blood pressure waveform [9]

For the blood to flow continuously through the cardiovascular system the arteries are storing up blood thanks to "Windkessel" effect. This is due to the viscoelastic properties of conduit arteries, which are keeping the blood pressure at the diastolic pressure level thus maintaining a continuous flow unlike if the system was stiff and with each systole, there would be a wave of blood inflow and at each diastole, the system would be still. The viscoelastic properties of the artery are based on its structure consisting of elastin, collagen and smooth muscle fibres [9].

Different pathological conditions can affect the structure and viscoelastic properties leading to change in PP culminating to CVDs. For example, arterial stiffness would lead to an increase in systolic pressure and a decrease in diastolic pressure leading to an increase in pulse pressure (also known as true systolic hypertension). Some conducted studies have shown that the risk of CVDs is much higher if the pulse pressure is very high e.g. 170 mmHg and 70 mmHg (SBP and DBP) in contrary to diastolic pressure being already high and the pulse pressure being lower e.g. 170 mmHg and 110 mmHg [4]. In the following table are given the normal and pathological levels for diastolic and systolic blood pressure

Table 1: Systolic and diastolic blood pressure values [10]

Blood pressure category	Systolic [mmHg]		Diastolic [mmHg]
Normal	less than 120	and	less than 80
Elevated	120 - 129	and	less than 80
Hypertension stage 1	130 - 139	or	80 - 89
Hypertension stage 2	140 - 180	or	90 - 120
Hypertension crisis	higher than 180	and/or	higher than 120

2.1.4 Central arterial blood pressure and amplification phenomenon

Central arterial blood pressure is the pressure at the ascending aorta on leaving the left ventricle. In the systole, it defines the work that the left ventricle has to perform maintaining adequate stroke volume. In the diastolic phase, it affects the regular blood flow to ventricular myocardium as the myocardial vessels are in systole compressed [9].

As stated in the previous section, the MAP is relatively steady throughout the arterial tree. The diastolic pressure has a minor change throughout the arterial tree descending about 1 mmHg to the brachial artery from the ascending artery. Systolic pressure on the other hand rises about 15 mmHg on average in the brachial artery and even more on the further peripheral arteries [4]. This is called the amplification phenomenon of arterial pressure (figure 3) and is caused by wave reflections.

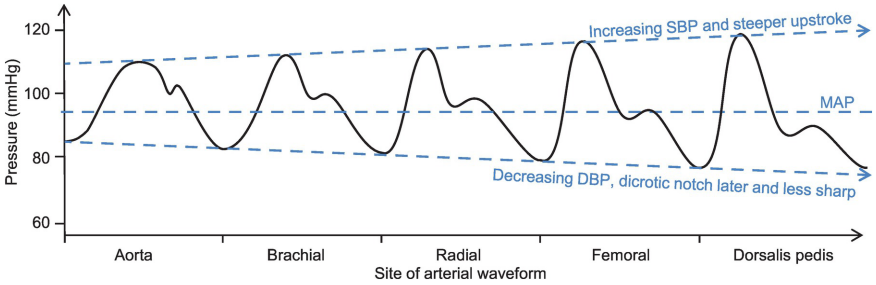

Figure 3: The amplification phenomenon of arterial pressure [9]

First, we need to mention the features of the circulatory system. It is a small-sized closed circuit, with quickly propagating pressure waves (about (4 to 19) m/s [11]). This causes the reflected backward waves to superimpose on the same forward wave that generated them. Thus, having a great effect on the whole pressure waveform especially the magnitude. The blood pressure wave is therefore the sum of the for-

ward (centrifugal) pressure wave and the backward (centripetal) pressure wave. The magnitude of a reflected pressure wave may be the magnitude 80-90 % of the forward wave [4].

These reflected waves arise in Arterial bifurcations, terminal arterioles defining the systemic vascular resistance, at narrowings caused by atherosclerotic diseases, or at obstructions in the arteries. On the bifurcations (the branching of the arteries) the forward wave splits into smaller forward waves related to the angle and calibre of the secondary branches and a backward wave is generated. One of the biggest bifurcations called the arterial bifurcation can be found in the pelvic area. Narrowing and obstructions caused by atherosclerotic diseases damp the magnitude of the forward wave and reflect a backward wave. But the major reflecting site is at the precapillary arterioles defining SVR [8]. Because of the sudden narrowing, we can observe a major pressure drop, as predicted in Hagen-Poiseuille law (equation 3).

$$\Delta P = \frac{8\eta l Q}{\pi r^4} \qquad [\text{Pa}] \tag{3}$$

Where ΔP is a pressure difference, η fluid viscosity, l length, Q flow rate and r radius.

On the peripheral arteries, the pressure is very much defined by the presence of wave reflection. We can observe a great influence of the superimposition on the forward wave. Because we are close to the reflection sites the superimposition affects early on the main pressure peak and the systolic blood pressure values. As in the central blood pressure, the wave reflection travels for a long distance with a delay to superimpose. Therefore, not affecting the systolic pressure peak or the systolic phase of the waveform, which is in the central blood pressure given mainly by the forward wave and the left ventricle aorta interaction. Instead, as it comes to the end of the systolic phase, the superimposition is prolonging the diastolic phase of the waveform, therefore ensuring good coronary blood flow [4].

With a lower pressure peak, the work needed to be done by the left ventricle can be kept low and the perfusion on the end of the arteriole is thanks to the high-pressure peak very effective. The amplification phenomenon helps to keep the ratio between cardiac work and peripheral perfusion as low as possible, to least the cardiac effort of the heart, which is to work for about hundred years and maintain the proper distribution of oxygen and nutrients on peripheries. This peripheral perfusion, the heart workload and the heart blood perfusion are very much affected by viscoelastic

properties, magnitude and variability of the reflected waves, length of the aorta, heart rate and the attenuation phenomenon of pressure waves [4]. Therefore we can predict CVDs from the pressure waveform.

2.1.5 Suprasystolic pressure

Suprasystolic pressure is higher than (20 to 40) mmHg than systolic blood pressure. By inflating a cuff to suprasystolic pressure a complete closure of the brachial artery occurs and there is no blood flow. This closure becomes a reflection site where we can measure the pulses of a directly reflected forward wave and later assess other hemodynamic parameters [12]. We have used this principle in our system.

2.2 Cardiac output

Cardiac output is the volume of blood that is pumped through the heart in one minute. It is defined as stroke volume times the heart rate and it is measured in litres per minute(equation 4). If the subject is calm and in normal physiological conditions a usual CO is about (4 to 6) l/min, although under stress or during intense exercise this number can rise to 20 l/min, because of the higher demand on oxygen and nutrients in the body [13].

$$CO = SV \cdot HR \qquad [\mathrm{L/min}] \tag{4}$$

There are several ways of measuring CO. The most accurate are invasive methods using a catheter, which either measures dilution of an indicator or the change in temperature after injection of cold physiological saline solution. A non-invasive way is using ultrasound and doppler effect. Thanks to ultrasound it is possible to measure the diameter of the artery and through the doppler effect, the blood flows in it thus directly measuring the stroke volume of the left ventricle [13]. Several other non-invasive methods are trying to compute the CO from different parameters like the Finapres®.

The Finapres® is a device using a finger clamp fitted with photoplethysmograph (PPG) and an inflatable finger cuff. This system allows maintaining constant blood

volume in the finger thanks to the inflation controlled by the PPG signal. The system is continuously measuring the pulse waveform and computing the HR and BP levels. The stroke volume is estimated from the arterial pressure-flow wave, aortic cross-section, age, gender, height, weight and body mass [14]. The results in testing for this device advice that the CO algorithm isn't very reliable a needs further adjustments, but the measurements of HR and MAP are reliable [15].

A novel way of CO monitoring is the pulse index continuous cardiac output (PiCCO) monitor. It is based on two methods. The arterial pulse contour analysis, which is continuously monitoring the blood pressure through a catheter in the femoral artery and is calibrated through transpulmonary thermodilution. It uses a similar algorithm for calculation of SV from the arterial pressure-flow wave, but the parameters are calibrated through the transpulmonary thermodilution thus fitting the algorithm for a precise CO measurement [16].

2.3 Pulse wave velocity

Unlike blood flow, which is on the order of cm/s PWV with ranges of (4 to 19) m/s is the simplest way to measure arterial stiffness (rigidity of the arterial wall) in a specific segment. The velocity of the pulse wave transmission is inversely related to the viscoelastic properties of the arteries, which are dependent on their composition (elastin and colagen fibres and smooth muscle) and health condition [17] and the arterial stiffness expresses the the instantaneous slope of the pressure–volume relationship (equation 5) [18].

$$PWV = \sqrt{\frac{V \cdot \Delta P}{\rho \cdot \Delta V}} \qquad [\mathrm{m/s}] \tag{5}$$

Where V is volume, ΔP is change in pressure, ρ is blood density (1.059 kg/L) [19].

Simply, we could count the PWV by capturing pressure waveform on a proximal and a distal site in the arterial tree (figure 4) and assessing the PWV from the distance of these two sites and the delay of the waveform (equation 6). While measuring the distance it is suggested to measure with a stiff rod and in the best case to measure the distance of the sites as the difference between the cardiac distances as opposed to the direct distance. To determine the delay, we measure the time from the foot of the pressure waveform. The foot can be identified through estimation of the intersection of the horizontal line tangent to the lowest point of the pressure waveform with the

prolongation of the straight line that minimizes the standard deviation of the points building up the initial proto systolic rapid ascending phase of the pressure waveform curve. Also, an algorithm based on a derivative of the change in arterial wall motion secondary to pulse pressure can be used [4]. For our solution, we decided to count the PWV from the time delay of the reflected wave and the forward wave and the distance of the Aorta and the bifurcation in the pelvic area.

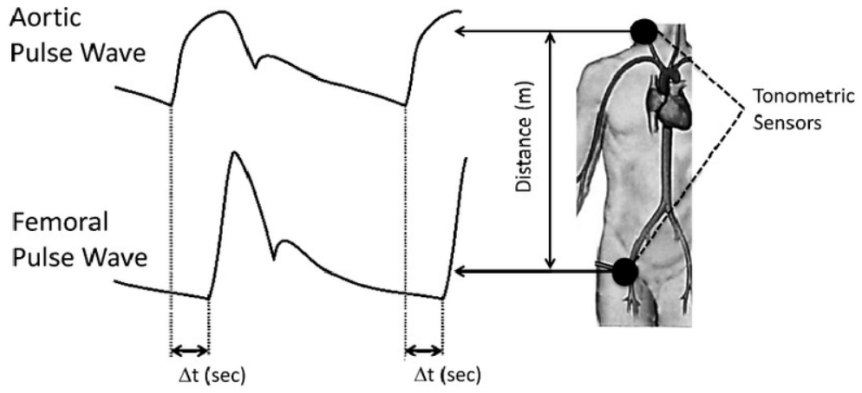

Figure 4: Measurement of PWV [20]

$$PWV = \frac{D}{\Delta T} \qquad [\text{m/s}] \tag{6}$$

Where D is distance and ΔT is time delay.

Let's introduce the terms distensibility and compliance. Distensibility is defined as the percentage variation in diameter of the artery for each increase in blood pressure of 1 mmHg (equation 7) [21]. Compliance is also closely related to the viscoelastic properties of the arteries and the Young modulus of elasticity. It shows the ability of vessels to be filled with blood(hold certain volumes) under different levels of pressure (9). It can be derived directly from PWV (equation 5) [22].

$$Distensibility = \frac{D_s - D_d}{D_d \cdot \Delta P} \qquad [1/\text{mmHg}] \tag{7}$$

Where D_s is end-systolic diameter of artery, D_s is end-diastolic diameter and ΔP is maximum pressure difference (pulse pressure). Further we can view distensibility as

the variation of Volume and insert it in equation 5, thus we will get the following equation(equation 8)

$$PWV = \sqrt{\frac{1}{\rho \cdot Distensibility}} \qquad [\text{m/s}] \tag{8}$$

$$C = \frac{\Delta V}{\Delta P} \qquad [\text{L/mmHg}] \tag{9}$$

As mentioned before the PWV is measured for a specific segment. Commonly measured segments are the carotid-femoral (cfPWV), brachial-ankle (baPWV) and the heart-femoral segment (hfPWV)[23]. For CVDs the cfPWV proved to be a reliable resource of conducting diagnosis and became a standardised measurement of PWV (figure 4). The measuring procedure is described in a previous paragraph where the proximal site is the carotid artery and the distal site is the femoral artery. It is sometimes also called aortic PWV (aPWV) [24].

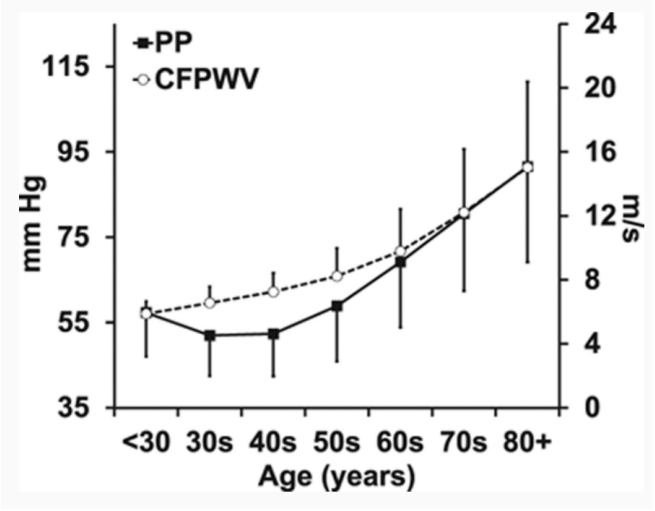

Figure 5: Mean values of PP and cfPWV according to age [25]

PWV depends on structural alterations and transient functional changes in the arterial wall. Structural alterations are often age-dependent where the elastin collagen fibre ratio changes. Elastin starts to degenerate and there is a boost in collagen, although the relation with age is not linear (figure 5). Other structural changes are caused by hypertension, metabolic diseases and inflammations. Functional changes are changes in MAP, left ventricular ejection time and smooth muscle cell tone. All these changes

are often leading to arterial stiffness. Another pathology is atherosclerosis usually caused by calcification, diabetes, metabolic failure, hypertension, kidney/liver failure, oxidative stress, inflammation and thrombi[26]. Reference values and conditions for PWV are shown in table 2.

Table 2: PWV reference values and conditions [23]

PWV (m/s)	Condition:
Less than 7	Optimal
7 - 10	Normal
10 - 12	High risk
Higher than 12	Abnormal

2.4 Parameters and indexes derived from the pressure waveform

From the pressure waveform, there are many parameters we can examine. Again it is very important on which site the parameters have been captured. In figure 6 we can see the pressure waveform of central arterial blood pressure captured at the aorta. Further in table 3 there are most parameters we can acquire and derive from the central blood pressure waveform.

Table 3: Parameters of central blood pressure [4]

cSBP	Central systolic blood pressure	The maximum blood pressure value in systole
DBP	Diastolic blood pressure	The blood pressure in end-diastole
cPP = cSBP - DBP	Central pulse pressure	The pulse pressure, i.e., the systo-diastolic change in arterial pressure
ESBP	End-systolic blood pressure	The blood pressure value at the end of systole
Ti	Travel time of the reflected wave	The time delay of the backward waveform, corresponding to Pi
Pi	Blood pressure at inflection point	The blood pressure value corresponding to the point where the backward wave starts superimposing onto the forward wave
AP = cSBP - Pi	Augmented pressure	The increase in blood pressure due to the earliness of the backward wave
AIx= 100 x AP / cPP	Augmentation index	The percentage increase in blood pressure due to the earliness in the backward wave with regard to the pulse pressure
Ar = AP / (Pi - DBP)	Augmentation rate	The percentage increase in blood pressure due to the earliness in the backward wave with regard to the forward pressure

In the next figure 7 another pressure waveform is shown with its parameters. These parameters can be measured on any distal measuring site and we can further derive the parameters shown in the table 4.

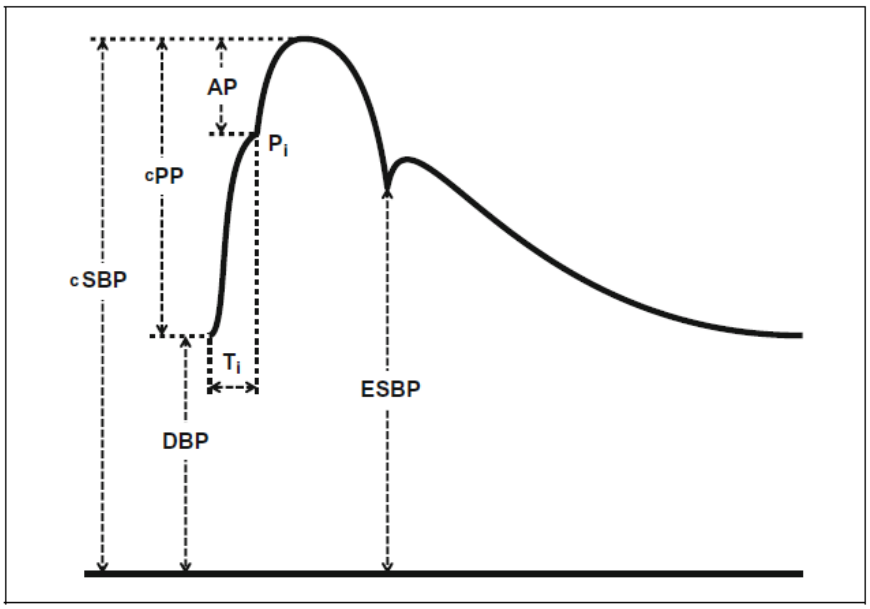

Figure 6: Pulse wave analysis of central blood pressure [4]

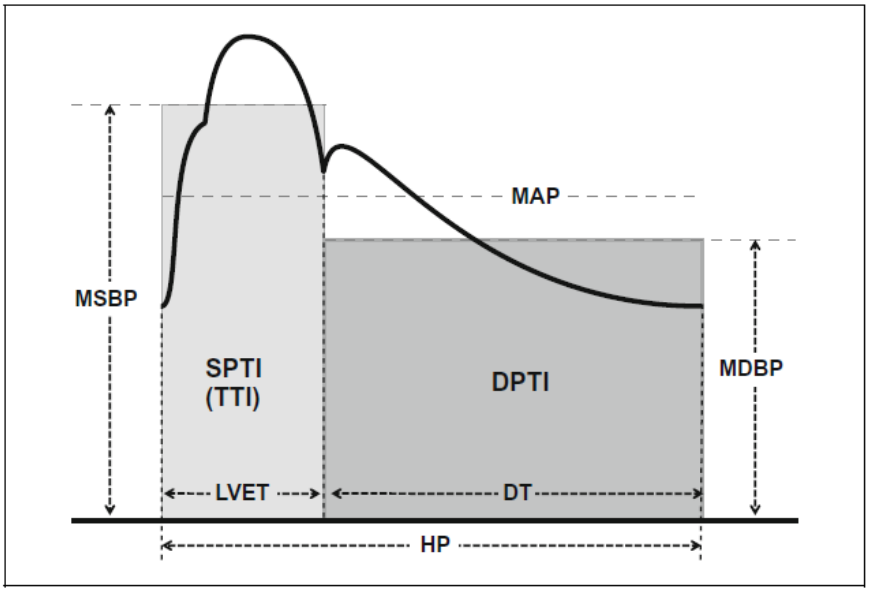

Figure 7: Pulse wave analysis on distal site [4]

Table 4: Pulse wave analysis parameters [4]

MAP	Mean arterial pressure	Mean of the single instantaneous blood pressure values
MPP = MAP - DBP	Mean pulse pressure	Mean of the single instantaneous pulse pressure values
MSBP	Mean systolic blood pressure	Mean of the single instantaneous blood pressure values during systolic phase
MDBP	Mean diastolic blood pressure	Mean of the single instantaneous blood pressure values during diastolic phase
LVET	Left ventricular ejection time	Duration of the systolic phase
DT	Diastolic time	Duration of the diastolic phase
HP	Heart period	Duration of the cardiac cycle, corresponding to the R0-R0 interval of ECG
DTF = DT / HP	Diastolic time fraction	Diastolic time as a fraction of the heart period
SPTI (TTI) = MSBP * LVET	Systolic pressure–time index (tension-time index)	Area subtending the systolic phase it represents the myocardial oxygen demand
DPTI = (MDBP - LVDP) * DT	Diastolic pressure–time index	Area included between pulse wave in ascending aorta and pressure wave in left ventricle in diastole (LVDP); it represents the myocardial oxygen supply
tonoDPTI = MDBP * DT	Tonometric diastolic pressure-time index	Area subtending the diastolic pulse wave; it is basically a DPTI which does not take ventricular diastolic pressure into account
SEVR = DTPI / SPTI	Subendocardial viability ratio	This index represents the balance between subendocardial oxygen supply and demand
tonoSEVR = tonoDPTI /SPTI	Tonometric subendocardial viability ratio	Ratio between the areas subtending by diastolic and systolic pulse wave; it is basically a SEVR which does not take ventricular diastolic blood pressure into account
Ampl. = pSBP - cSBP	Amplification phenomenon (mmHg)	Difference between systolic blood pressure values measured in the brachial artery (pSBP) with respect to systolic blood pressure values in the ascending aorta (cSBP)
PPA = (pPP - cPP) / cPP	Pulse pressure amplification (%)	Percentage increase in pulse pressure values measured in the brachial artery (pPP) with respect to pulse pressure values measured in the ascending aorta (cPP)
FF = MPP / cPP	Form factor	Ratio between mean pulse pressure and pulse pressure; it is an attempt to “quantify” pulse waveform

2.4.1 Augmentation Index

The augmentation index (AIx) is another parameter that proved to be useful in CVDs diagnosis, indicating the superimposition of a reflected wave on the forward wave and the incidence on the total pulse pressure [27]. AIx is defined as the ratio of augmented pressure (AP) and pulse pressure(PP) (equation 10). Where the augmented pressure is derived from the difference of the central systolic blood pressure and the inflexion point of the blood pressure (as seen in figure 6). The inflexion point can be before or after the systolic peak causing the AIx to be either positive or negative. This allows us to have AIx concerning the timing of reflected waves [4].

$$AIx = 100 \cdot \frac{AP}{PP} \qquad [\%] \tag{10}$$

Corresponding to the point where the forward and backward wave meet is the inflexion point, in most cases it can be easily spotted but in some cases, we can find this point in the fourth derivative of the pulse wave on the zero-crossing after the highest positive peak (figure 8) [28].

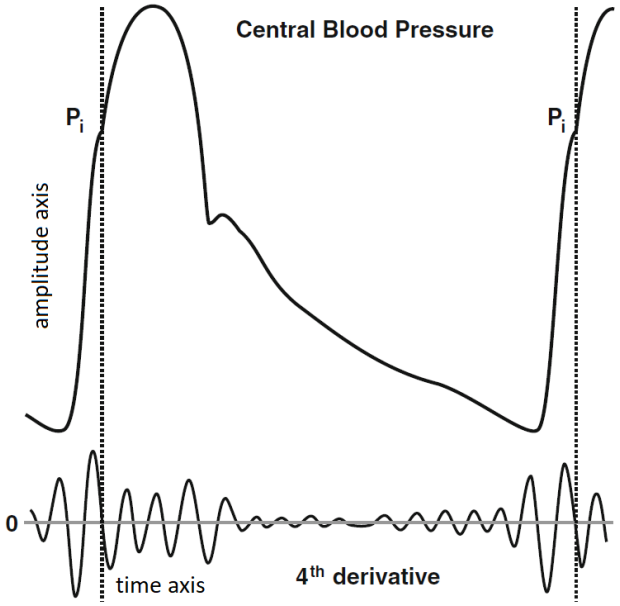

Figure 8: Detection of the inflection point from the 4th derivative [29]

Similarly to central blood pressure, AIx is highly dependent on many factors such as gender, age, height, systemic vascular resistance, viscoelastic properties and arterial stiffness. Again the site plays also an important part since the augmentation phenomenon tends to have a higher effect on the peripheral arteries [29].

2.4.2 Form factor

The parameter form factor (FF) helps to quantify the different pulse waves. It is defined as the ratio between mean pulse pressure (see table 4) and pulse pressure (equation 11) [29].

$$FF = \frac{MPP}{PP} \qquad [-] \tag{11}$$

The central pulse waveform can be also classified by the Murgo–Nichols classification, this classification distinguishes four different waveform types on the earliness of the backward waves [30]. The parameters of the waveform types are shown in table 5 and the waveforms are shown in figure 9.

Table 5: Murgo–Nichols classification of central pulse waveform [29]

Type:	AIx [%]	Timing of reflected waves	Age [years]	Diastolic waveform
A	>12	Protosystole	>40, <65	Concave
B	>0, <12	Mesosystole	>30, <40	Convex
C	<0	End-systole	<30	Concave
D	>>12	Early protosystole	>65	Convex

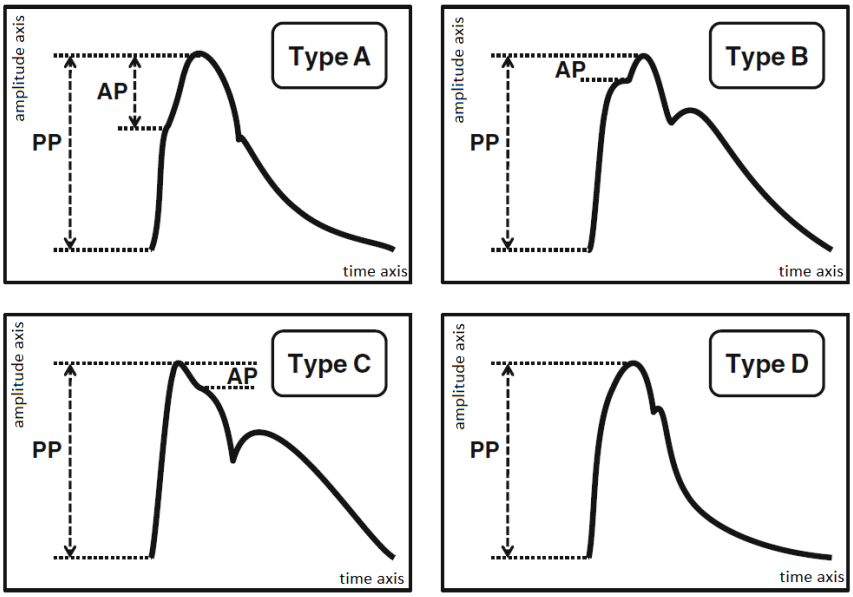

Figure 9: Murgo–Nichols classification of central pulse waveform [29]

2.4.3 Pulse pressure amplification

As mentioned in the section Central blood pressure, the pulse pressure in the peripheral arteries is much higher than in the ascending aorta thanks to the amplification phenomenon and the short distance of the reflection sites causing the backward wave superimposing on the systole of the forward wave. A significant association between CVDs and low pulse pressure amplification has been found (figure 10) [31].Pulse pressure amplification (PPA) defines the percentage increase in pulse pressure values measured in a peripheral (often brachial) artery with respect to central pulse pressure values (equation 12) [31].

$$PPA = 100 \cdot \frac{pPP - cPP}{cPP} \qquad [\%] \tag{12}$$

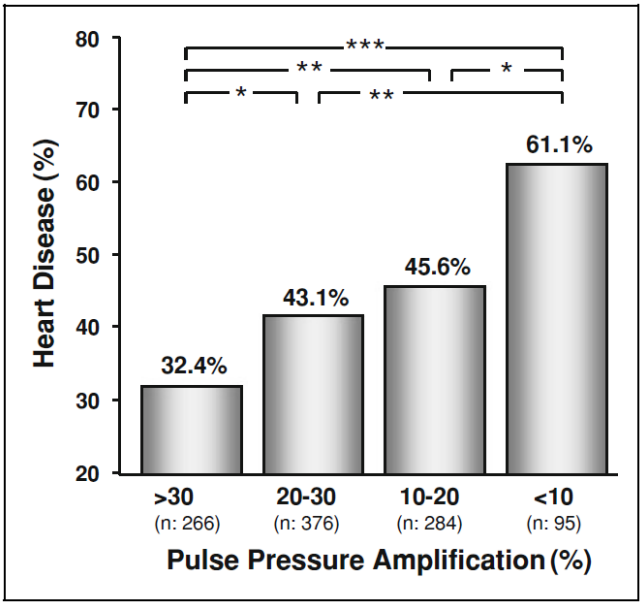

Figure 10: Relation between CVDs and PPA, * P<0.01, ** P<0.005, *** P<0.001. Outcomes of the PARTAGE study [29]

2.4.4 Subendocardial viability ratio

Another useful indices for cardiovascular risk, particularly coronary artery disease, is the subendocardial viability ratio (SEVR), also known as the Buckberg index. SEVR is the ratio between myocardial oxygen demand and supply (equation 14) [29].

$$SEVR = \frac{DPTI}{SPTI} \qquad [-] \tag{13}$$

Where $DPTI$ is the diastolic pressure time index, which represents the myocardial oxygen supply (the area between pulse wave in ascending aorta and pressure wave in the left ventricle) and $SPTI$ is systolic pressure time index representing myocardial oxygen demand (area under the systolic phase) (figure 7). These phases are separated by the dicrotic notch [32].

2.5 Estimation of central blood pressure from brachial blood pressure

Central (aortic) pressure is a key component for deriving many indexes and indicate CVDs. Therefore it is a parameter we would like to measure. The most common method is an invasive measurement with a catheter inserted directly into the aorta through the femoral or radial artery. This method is the most precise, but it comes with certain drawbacks since the invasive method requires surgery. Different methods have been examined for a noninvasive approach. The aorta is in a difficult measurable area so the newest approaches are focusing on requiring the Central blood pressure from different peripheral sites such as the brachial artery or the femoral artery. Several methods using a cuff inflated to suprasystolic pressure and using a transfer function based on a model have been tested with promising results [12]. One of these methods has been devised by the company AtCor. The system called SphygmoCor®. This system uses a combination of ultrasound and a pressure cuff and can measure the PWV, the pressure waveform and to compute the central arterial pressure [33]. There have been also attempts at using only the cuff on brachial artery inflated to suprasystolic pressure. These methods require an estimation of parameters which can be done with brachial tonometry or with an invasive measurement showing much better results.

One of these methods assumes that the only needed parameters for the transfer function are the wave propagation transit time and the reflection coefficient at the cuff. Using the suggested method (equation 14) the estimates of central pressures exceed the requirements of AAMI SP10 (requiring agreement better than (5 ± 16) mmHg), showing (figure 11) a promising result and requiring further examination [34].

$$P_{t0}(t) = \frac{b}{b+1} P_{t3}(t - dt) + \frac{b}{b+1} P_{t3}(t + dt) \qquad \text{[mmHg]} \tag{14}$$

Where P_{t0} is total oscillatory pressure in the aorta, P_{t3} is total oscillatory pressure under the essentially occluding cuff, t is the time variable, b the reflection coefficient for a pressure wave travelling distally at the cuff, and dt the time taken for a pressure wave to travel from the subclavian root to the cuff occlusion [34].

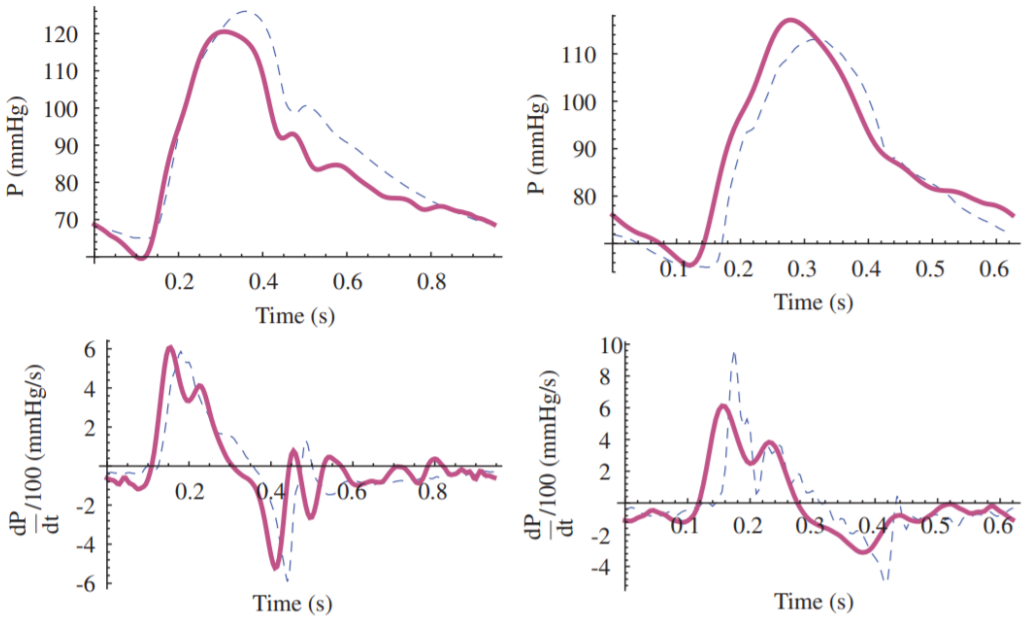

Figure 11: Examples of two reconstructed (solid) and actual (dashed) central pressure waveforms. Pressure (top) and first derivative of pressure (bottom) are shown [34].

3 Research of hardware and software tools

3.1 Raspberry Pi

When choosing the hardware platform for a project there are many things to take into account. Our system had to be able to register data, to analyse and compute the data and to be able to interact with the user through a touch display. For this purpose, we have decided to use the Raspberry Pi platform.

Raspberry Pi is a single-board microcomputer running a Linux based operating system. It is being powered by an ARM processor and has enough RAM to run multiple programs at the same time. The Raspberry Pi platform offers several models of its microcomputer with different levels of processing power and means of connectivity. The similarities between these boards are that they are run by an ARM-based processor, they have integrated RAM and a micro SD card slot for storage. Also, they are equipped with GPIO pins which allow several functionalities listed in the section below. Between other inputs and outputs that are model specific are USB ports, HDMI port, 3.5mm audio jack, Wi-Fi, Bluetooth and ribbon connectors for camera and display (figure 12) [35].

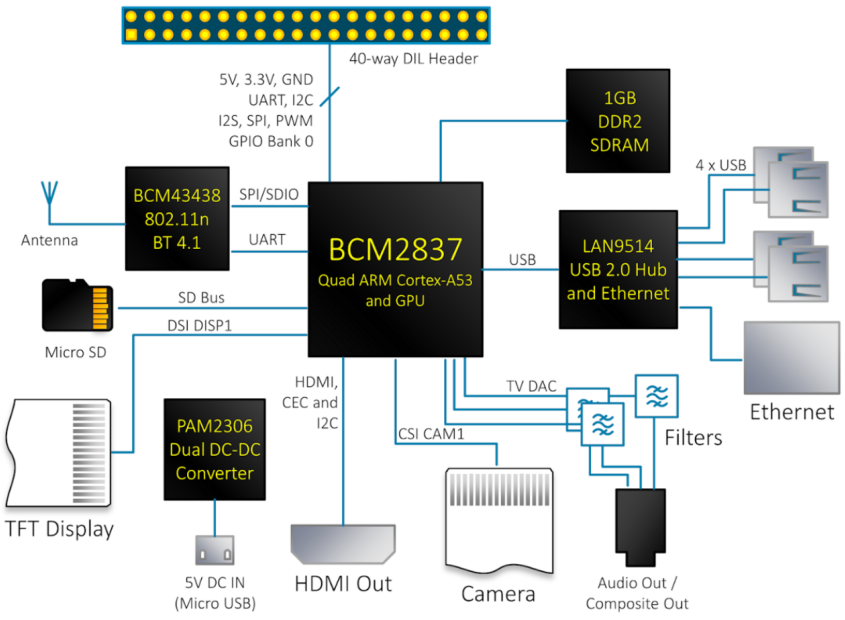

Figure 12: Block diagram of a Raspberry Pi microcomputer [36]

3.1.1 Power requirements

To power up a Raspberry Pi board, we need a 5V stable power supply. The typical bare-board active current consumption is between (150 to 600) mA. The easiest way to power up the RPi is to use a USB charger or connecting to a power bank with a USB to micro-USB cable, thanks to the boards micro-USB port with a PAM2306 DUAL DC-DC converter. Different ways require a stable 5V voltage. This can be achieved through a linear stabilizer, which can have high consumption but offers high stability with low noise. Another way is to use a DC to DC convertors such as a boost or step-down convertor, these use a very fast switching frequency which may cause noise in some application but are power efficient. The stable voltage supply can be then directly plugged into the GPIO ports and power up the board. Raspberry Pi boards also offer a 3.3V output thanks to the integrated DC-DC converter. The boards will automatically start and boot to the installed OS when plugged into the supply. As there might be loss of data and corruption of system files with a power outage, the system needs to be properly shut down through the OS [35].

3.1.2 GPIO

Depending on the model the RPi board offer either 26 or 40 pin headers (figure 13). Between these headers, we can find 5V and 3.3V power headers which can supply up to 1.2 A and ground headers. Some pins can have specific functionalities such as PWM, SPI and I2C serial ports. All GPIO pins are equipped with pull up resistors which can be set through software [35].

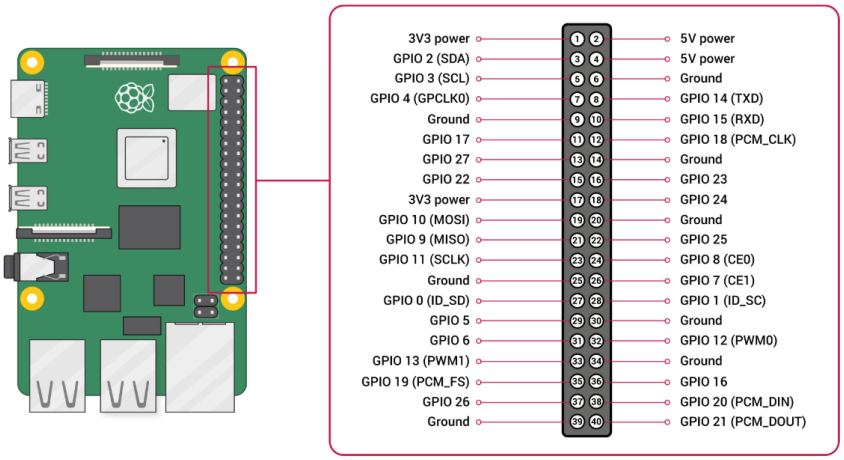

Figure 13: GPIO pins of a Raspberry Pi microcomputer [35]

3.1.3 Operating system

Raspberry Pi is capable of running several Linux based operating systems, which allow easier communication between the end-user, software and hardware and allows us to run programs. Depending on the application of the system we can choose the process, device, file, input/output, storage and memory management capabilities of the OS. For a very specific application of the Raspberry Pi, we want to have a fast booting OS that is running only the essential management for the application, without wasting processing resources and power.

The recommended OS for Raspberry Pi is the Raspberry Pi OS (formerly Raspbian). it is a free Debian based OS optimised for the Raspberry Pi hardware [37]. It has an LXDE (Lightweight X11 Desktop Environment) desktop environment that allows an intuitive and easy to use management of the system maintaining low resource requirements [38]. It comes with a lot of preinstalled programs for the development of your projects in a multitude of programming languages such as Python, C or Java, an office suite and a web browser and is capable of running multiple programs in parallel and separate windows on one screen thanks to the Openbox window manager [39]. Currently, there are two versions of the Raspberry Pi OS available with the option of installation with the recommended software. The second version is a Lite version that comes with a headless environment and without any preinstalled software using as few resources and storage space as possible. The desktop version od Raspberry Pi OS uses

up to 1128 MB of storage whereas the Lite version takes 432 MB, the recommended software takes additional 1395 MB [40].

Another lightweight OS is DietPi, it is also based on Debian and is available also for several other single-board computers. The storage requirements are at 589 MB. Its distinct features are high optimisation for minimal CPU (core processing unit) and RAM (random access memory) resource usage, logging system choices, software priority level control and automation capabilities. It also comes with a desktop interface and preinstalled software for development [41].

There are many other OSs than can be used with Raspberry Pi computers. some of them are used for a specific application like media or data servers and some allow a broad spectrum of usage like the previously mentioned Debian based systems. Many OSs are now used for IoT (internet of things) systems such as Windows IoT or Ubuntu IoT. We have been using the Raspberry Pi Os with its desktop environment since it was helpful in the development of the software used in the Raspberry Pi.

3.2 Python

There are many options for choosing a programing language when writing your software code. Some languages are more often used in specific scenarios for example MATLAB in Signal Analysis and scientific use or C in microcontroller programming. Since we have been working on a system that involves different kinds of software implementation, our goal was to use a language capable of doing all the needed tasks. These tasks were implementing a GUI, controlling a Pneumatic system, reading the measured data and analysing the measured data. Since raspberry pi offers great support for Python, is commonly used in software and web applications and is already preinstalled on Raspberry Pi we decided to use Python as the language for our applications.

Python is a high-level dynamic programming language ideal for quick programming tasks and rapid application development on many platforms. It is using an intuitive syntax and suggests using object-oriented programming thanks to its simple and effective approach. Because it is an interpreted language it allows for application development across many platforms and in many areas, from small projects to web applications and their infrastructure. Python is a free open source software with freely available source code. Therefore there is a huge community of developers creating free packages that can be used to accomplish nearly any task [42].

For GUI creation many frameworks for many languages exist, many of them can be used across different platforms. For example, the Qt library with its Python toolkit PyQt can be also used with C, C++, Ruby and Java [43], Commonly used with Python is the TkInter framework. Because we wanted to use our device with a touchscreen we decided to use the Kivy framework with Python which allows us to use a multitude of touch inputs [44].

For hardware programming often the C language or its extensions are used since it allows to communicate with the input-output interfaces on lower levels and doesn't need a longer interpretation of the code as other higher programming languages [45]. Anyhow, the Python libraries allow us to program and use the GPIO interfaces of the Raspberry pi through many libraries too, therefore we have implemented these libraries into our Python code.

For data analysis, we used many libraries that Python offers like SciPy, NumPy, Pandas and Matplotlib, which allowed us to properly analyze and view the measured data. In many scientific facilities and universities, we can come across the MATLAB programing language, which is a very useful language for data analysis, design process and scientific research. If we were to compare MATLAB with Python, Matlab is a closed source software that is licensed to use. Therefore sharing and using your code on different platforms or devices can be difficult since only devices with a MATLAB licence can use it. It is also exclusively developed by Mathworks and many toolboxes and libraries require further licencing [46].

4 Technical documentation

The system we have designed consists of two main parts, the pneumatic part and the electronic part. The core of the whole system is the Rasberry Pi and its software, that is controlling all the individual elements. In figure 14 we can see the two main parts and the block diagram of the system.

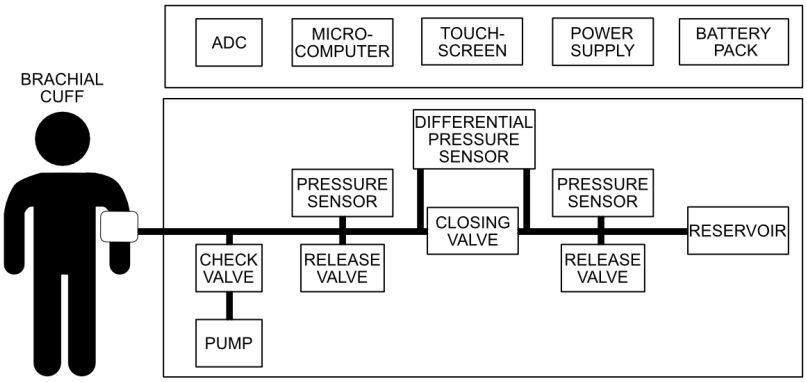

Figure 14: The Block diagram of the system

4.1 Pneumatic component

The pneumatic system allowed us to transduce the pressure signal from the brachial artery to our sensors. Few parameters were needed to accomplish for our system to work, like airtightness, low noise, good transfer of the signal, low energy requirements and safety of the system. The individual elements are connected with stiff Polyurethane tubes with an outer diameter of 6 mm and an inner diameter of 4 mm. Many elements were also put into a junction made out of machined aluminium. The pressure component is shown in the pneumatic circuit diagram in figure 15. All the individual elements are further described in the following section. The pneumatic component was based on an already existing system.

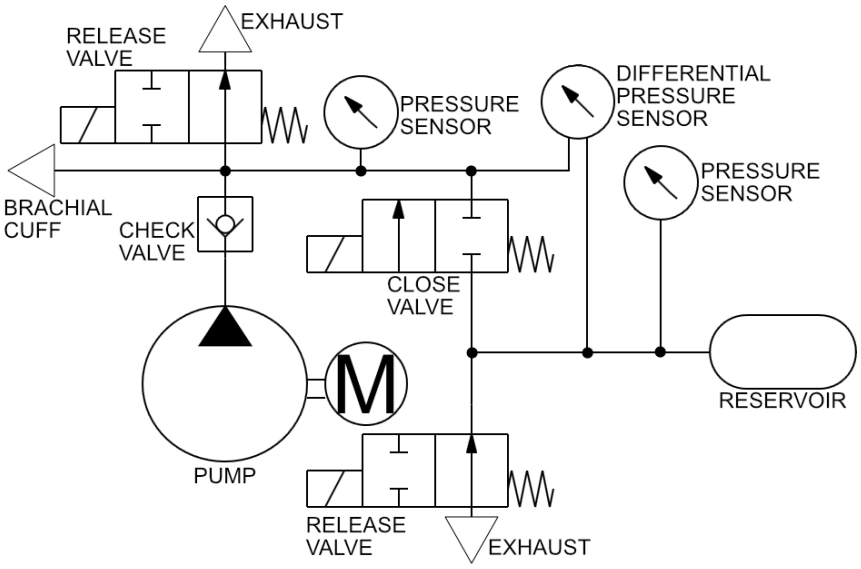

Figure 15: Diagram of the pneumatic circuit

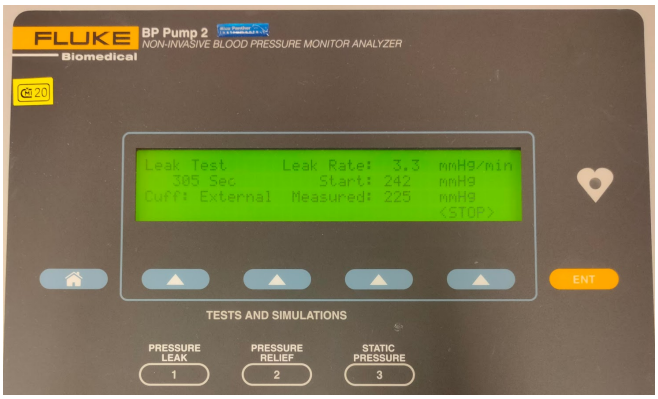

Figure 16: Pressure leak test using the Fluke BP Pump 2

We have performed a pressure leak test on a Fluke BP Pump 2 testing device to determine the airtightness of the pneumatic component, the test was run on the system with the closing valve closed and opened and was run for 300 s. With the opened valve the leak rate was 3.7 mmHg/min and with the closed valve the rate was 3.3 mmHg/min. The pneumatic component needed a few seconds to stabilize when inflated to a certain level of pressure. The leakage was small enough to perform proper measurements.

4.1.1 Pump

The pump we have used was a P54A-0002R air pump from OKEN SEIKO CO.,LTD.. It was based on an RF-370-C DC (direct current) motor rated at DC voltage 6 V with a minimum current of 180 mA and maximal current of 290 mA. The free flow of the pump was 1.8 L/min and the maximum pressure it could hold was 90 kPa (675 mmHg). The noise produced by the pump was about 48 dBA.

4.1.2 Valves

In our pneumatic system, we have used three active valves and one passive valve. The passive valve was a check valve used right behind the pump helping to avoid any pressure leakage through the pump. It was a duckbill valve commonly used in aquarium air pumps.

Two of the active valves were the release valves. One of them was on the cuff side, and the other on the reservoir side. The normally open release valves JQF4-6A were rated for DC voltage 6 V with linear voltage control and a current flow of 107 mA when closed. The maximum pressure they could hold was 350 mmHg.

The third active valve was a closing valve between the two sides. The closing Valve was a solenoid valve with a rated DC voltage of 5 V, power consumption was 1.2 W and the exhaust speed was 15 mmHg at 300 mmHg. The valve was normally closed and the leakage was rated at less than 1 mmHg per minute.

4.1.3 Reservoir

The reservoir allowed us to maintain a steady reference pressure to the suprasystolic pressure on the cuff side after the valve was closed, thus allowing the differential sensor to have accurate measurements within its measuring range. The first reservoir we used was a FESTO CRVZS-0,1 with a volume of 0.1 L, we couldn't find proper junctions for the reservoir and the junctions we made were leaking. Therefore, we used a homemade reservoir made of steel with a welded junction.

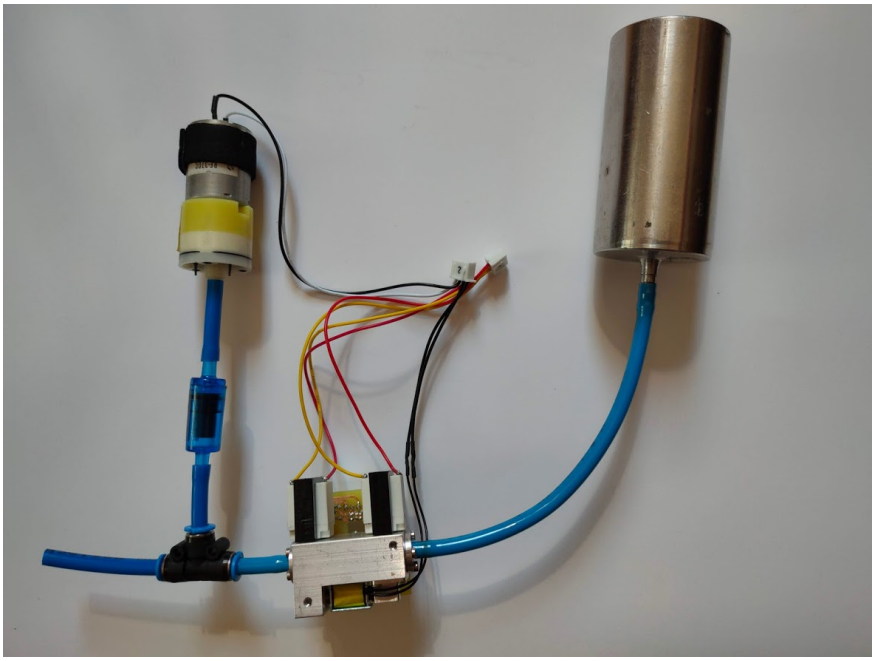

Figure 17: Picture of the pneumatic component, left: pump with check valve, centre: aluminium junction with sensors (on the PCB), closing valve (bottom) and release valves (top) , right: reservoir

4.2 Control component

4.2.1 Raspberry Pi

In our system, we have been using the Raspberry Pi Model 3 as the core of the system. The CPU of this microcomputer was a Quad-Core 1.2GHz Broadcom BCM2837 64bit processor with 1GB RAM. Further equipped with BCM43438 wireless LAN and Blue-

tooth Low Energy (BLE), 100 Base Ethernet, 40-pin extended GPIO, 4 USB 2 ports, 4 Pole stereo output and composite video port, full-size HDMI, CSI camera port, DSI display port, micro SD port and an Upgraded switched Micro USB power source with up to 2.5 A.

The OS we were running was the Raspberry pi OS with desktop and suggested programs. On the RPi were scripts for controlling and reading data from the system and analyzing algorithms to computation the hemodynamic parameters.

To control the release valves and pump we used a PWM (pulse wave modulation) signal of 200 Hz and for closing and opening the closing valve we set the output of a pin to either high or low.

Figure 18: Raspberry Pi mounted on the back of the touchscreen

4.2.2 Means of switching

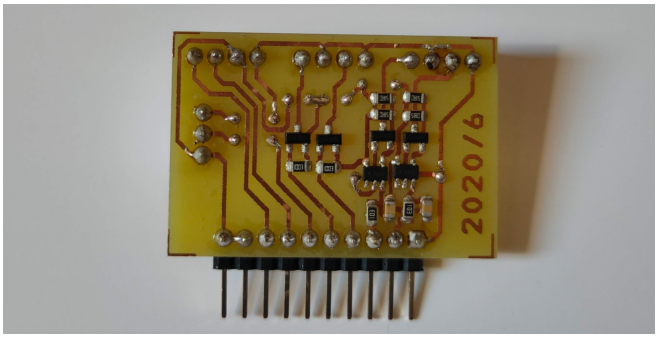

Figure 19: PCB with switching electronics

We used two types of switching for the pneumatic elements in our system. For the pump and the closing valve, we used BSS306N N-channel MOSFET transistors (figure 20), which were rated for logic levels of 4.5 V on Gate-Source, the continuous drain current of 2.3 A, and maximum Drain-Source voltage at 30 V. We used the PWM signal to adjust the speed of the pump and switch the high low levels to open or close the closing valve.

Since the release valves could be controlled by linear voltage control we needed to adjust the circuit in figure 20 to figure 21. We filtered the PWM signal with a low-pass filter with a cut-off frequency of 159 Hz. After that, the voltage is converted to current and the valves are linearly controlled by the current through the tranzistor.

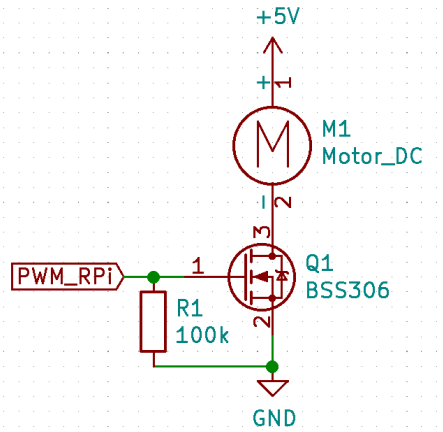

Figure 20: PWM switching of pump

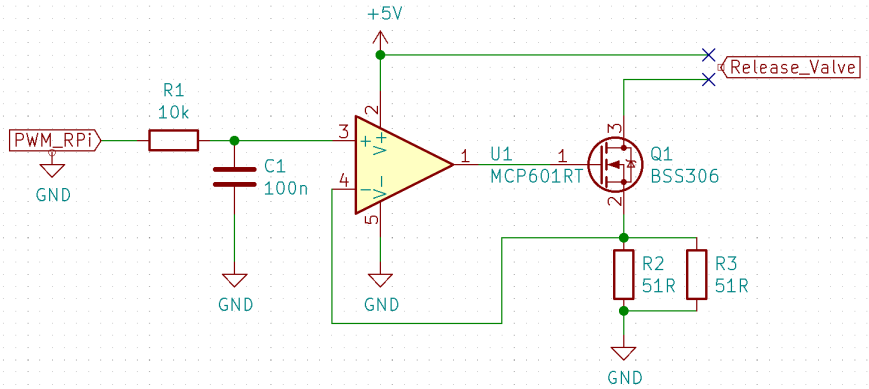

Figure 21: PWM switching with linear voltage control

4.2.3 Touchscreen

For displaying and user input we used the official Raspberry Pi Touchscreen which was a 7 inch LCD (liquid crystal display) with a resolution (800 x 480) pixels. The connection to RPi was made through the DSI display port. It was powered by 5 V DC. The capacitative touch layer allowed for up to 10-finger touch recognition.

4.3 Power supply

The system could be powered up by a 5 V DC 2.4 A micro USB charger. For a more portable solution and lower noise we first used a USB power bank. Later we used the BS301CV module made by LantianRC connected to 4 LGDBB31865 Li-Ion batteries with a capacity rated at 2600 mAh, nominal voltage at 3.7 V and a maximum voltage of 4.2 V each. The board allowed for charging with (4.65 to 5.5) V with a maximum current of 2.1 A and discharge at 5 V with up to 2.4 A current flow. It had an over-current, over-voltage, short-circuit and overheating protection. The efficiency of the DC to DC conversion was 96 %. Also, it was equipped with 4 LEDs (light-emitting diodes) to indicate the charge level by 25 % levels and was switched on and off with a button.

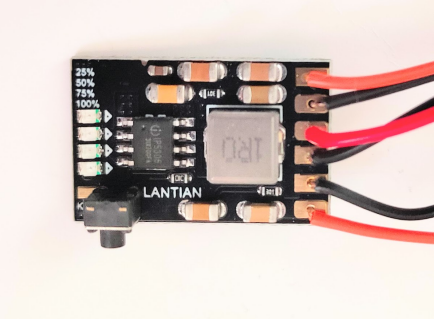

Figure 22: The BS301CV module for powering up the system

4.4 Measurement component

4.4.1 Sensors

In the system, we used two gauge pressure sensors and one differential pressure sensor. The gauge pressure sensors were again mounted on each side of the system, on the cuff side and the reservoir side and the differential sensor was mounted between the two separate parts, all in the aluminium junction.

The differential pressure sensor was a HSCDRRN002NDAA5 TruStability® board mount pressure sensor. It was rated at a DC supply voltage of 5 V, pressure range at ±2 inH_2O (around ±3.7 mmHg) and a maximum working pressure at 135 inH_2O (around 250 mmHg).

The two sensors were the MP3V5050GC6U analogue gauge pressure sensors. They were rated for a DC supply voltage of (2.7 to 3.3) V. Thus, a linear DC voltage regulator for conversion from 5 V to 3.3 V needed to be added. For this purpose, we used an LM3480/SOT low-dropout voltage regulator rated at maximum input DC voltage of 30 V and an output maximum current of 100 mA at 3.3 V. The current draw of one sensor was (7 to 10) mA and the working pressure was (0 to 50) kPa (up to 375 mmHg).

4.4.2 Analog to digital converters

Since the RPi didn't have a built-in analogue to digital converter (ADC), we needed to use a separate chip for the conversion. The RPi allowed for both I2C and SPI communication.

At first, we used the ADS1115 I2C ADC with 4 single-ended or 2 differential channels, a resolution of 16 bit and a maximum sample rate of 860 sps it used a $\Sigma\Delta$ convertor and was rated for supply voltage between 2.0 to 5.5 V. The consumption during the continuous conversion was 150 μA. However, the sample rate we wanted to achieve was at about 2000 sps and the communication between Raspberry Pi and ADS1115 we achieved was at a maximum of around 100 sps.

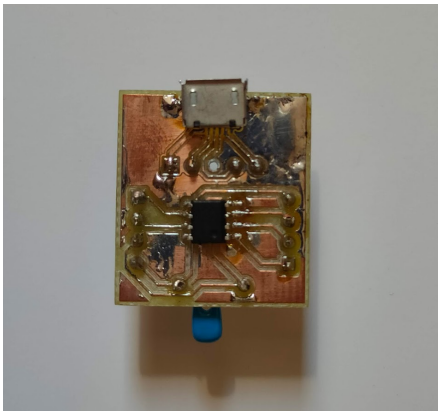

Figure 23: MCP3202 mounted on a PCB

Therefore we decided to use an SPI ADC. The MCP3202 had a 12-bit resolution and two single-ended or one differential channel. The conversion was made with successive approximation and a sample and hold circuit. The rated conversion rate was up to 100 ksps. The Supply voltage was (2.7 to 5.5) V with a maximum current flow of 550 μA. The ADC was mounted on a separate PCB (printed circuit board) and connected with wires to the sensors and RPi (figure 23).

4.5 Software

A key part of the system was the software running on the RPi. Mostly we used all scripts written in Python programming language, but we had to use also a script written in C language. The RPi was well adjusted to run all the scripts but several libraries were needed to be installed.

The scripts consisted of two parts, the blood pressure part and the PWV part. Each of these parts had a script for capturing the data, for controlling the pneumatic elements and for data analysis.

4.5.1 Control scripts

We decided to write the code for controlling the elements of the pneumatic part in Python and use a GUI written in Kivy framework to make it user friendly. The initialization of all the controlling scripts is similar for both the blood pressure part and the PWV part. The release valves had to be closed, the pump had to be shut and the closing valve had to be open. For the control of the pneumatic elements, we used the RPi.GPIO library.

For the blood pressure measurement, we initialized a PWM signal for the valves and pump at 200 Hz. The pump was run at 0 % and the valves at 100 % PWM signal. The closing valve was open by setting the output of the controlling pin to a high logic level. If the button "Inflate" was pressed the pump has started to inflate at 60 % PWM signal for 30 s, these values proved to be sufficient to inflate the cuff for most subjects to 200 mmHg. While the button "Release" was being pressed the release valve have had open, thanks to the PWM signal decreasing to 0 %. If the button was released the valves have had closed again. The button "Close/Open valve" was switching between the logic levels of the pin controlling the closing valve, thus closing and opening the closing valve. If the button "Exit" was pressed, the valves would release all the pressure and the script would shut down. The interface is shown in figure 24

For the PWV measurement, we have adjusted the previous script. We didn't need the PWM signal, since we needed to inflate the cuff to the suprasystolic level. Therefore we have initialized all the controlling pins to output high or low levels. The difference in

Figure 24: Control GUI used in the measurements

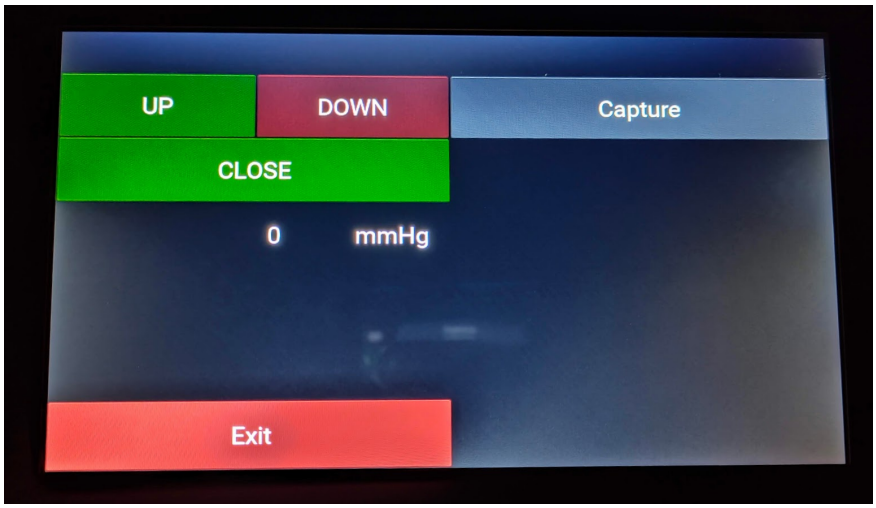

Figure 25: Control GUI with continuous values feed

this script was the change in the function of the "Inflate" button. While being pressed the pump have had run, and if the button was released the pump have had shut down again. The other buttons remained the same function. For this measurement, an aneroid sphygmomanometer was added to the pressure circuit at the cuff side to monitor the pressure levels.

We have attempted to create a GUI with continuous reading of the pressure values from the sensor. This GUI is shown in figure 25. The continuous reading was successful, but we also wanted to add the function of capturing the data by pressing the button "Capture", which made the script crash. The functions for the continuous read and capture were written in Python and are further mentioned in the next subsection. We have also changed some of the names of the buttons, instead of "Inflate" we have used "Up", instead of "Release" we have used "Down" and instead of "Close/Open valve" we have used just "Close/Open". The functions of the buttons remained the same to the ones used in PWV measurement.

4.5.2 Measurement scripts

Since we wanted to keep all the scripts in Python we have written several scripts implementing different libraries of Python for communication with the MCP3202. Most of these libraries weren't much adjustable and allowed for a slow sample read. We decided to use the "spidev" library and implement our communication with the ADC through SPI. First, we needed to initialize the SPI communication on the RPi with a clock speed of 1.8 MHz on channel 0. Then we created the "read_adc" function, which sends the 16 configuration bits to the ADC and receives 16 bits with the value written in the last 12 bits. The bits were transferred to an integer and returned by the function. In the before-mentioned GUI script implementing the continuous read, this function was always run during the renewal of the Kivy window. The function capture was to write the data in a .dat file with a delay 500 μs to achieve a sample rate of 2 ksps. The problems that occurred were that the renewal clock speed of Kivy didn't allow for such a fast conversion, and if run behind the Kivy script, The samples would have severely different time delays between the samples with some outages caused by the clocks of the different Python scripts interfering.

To tackle this problem we have written the script for data capture in C programming language. Which allowed us to communicate with the processor on a lower level than

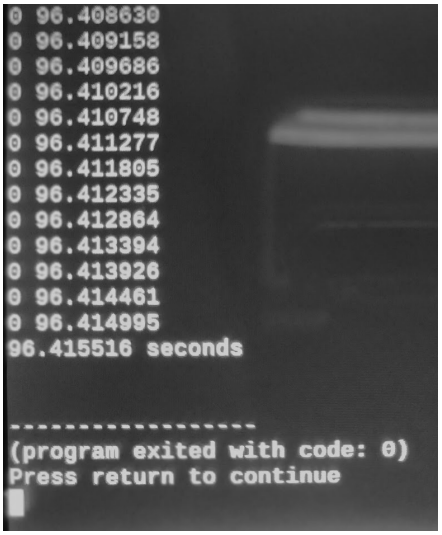

Figure 26: C script running in the background capturing data and time

an interpreted language like Python. For the C script, we used the "bcm2835.h" library. This library had already some function that made the SPI communication much easier. First, we initialized the SPI communication with the ADC and defined the configuration script. In a cycle of predefined samples, we have sent the controlling bits, received the sample, converted the sample into integer and recorded the sample and its timestamp into a .dat file, each of the runs of the cycle had a delay of 500 μs to achieve 2 ksps. This implementation proved to be working best since we didn't have any interference from other scripts and programs and the samples were taken with a delay varying only in dozens of μs. The script running in the background is shown in figure 26. The script was similar for both measurements except sending different configuration bits to read either from the channel connected to the pressure sensor or the channel connected to the differential pressure sensor.

4.5.3 Blood pressure analysis script

For the blood pressure analysis, we used libraries "numpy", "pandas", "matplotlib" and "scipy". First, we have loaded the data from .dat file, that had two columns, into arrays. The first column had the integers representing the values of pressure and the second column had the timestamps. From the timestamps, we counted the real sampling rate and the Nyquist rate. We made a new timeline with the sampling rate

and converted the integers from ADC to pressure values in mmHg. The parameters for conversion were acquired through a five-point calibration and linear regression. The loaded data is shown in figure 27.

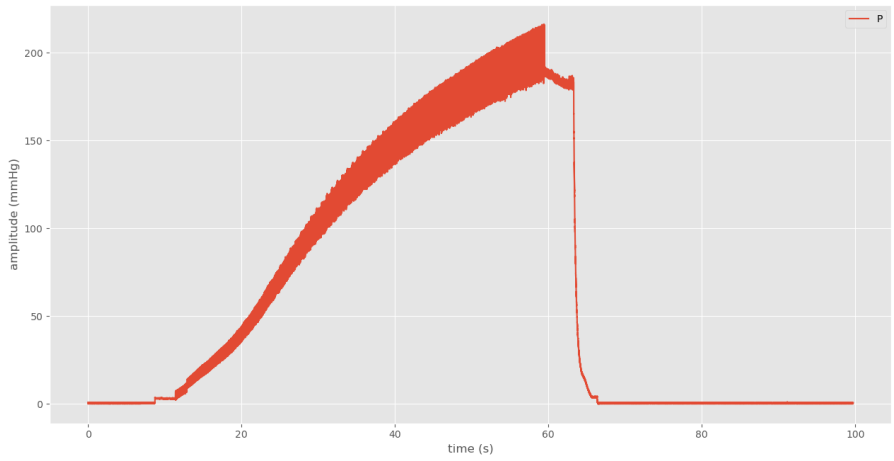

Figure 27: The raw signal

After that, we have filtered the data with a low-pass (LP) FIR (finite impulse response) filter with a cut-off frequency of 3 Hz, an order of 101 and a "hamming" window. The cut-off frequency was chosen through the spectrum magnitude of the signal, which showed that after 3 Hz, there was no useful signal. The data was shown in a plot. In this plot, the user had to choose the region of interest with a vertical span selector. Since we were assuming that the measurement will always start from a deflated cuff, the span selector chose the first highest samples equal to the selected span (figure 28). It was also assumed that the selection made would have been in the range of normal blood pressure eg. (50 to 200) mmHg if, on the other hand, the selected area was too small, the script would have cancelled in the next step. The selected region of interest is shown in figure 29. If the selected area was too small, the plot would be empty and the script would have cancelled.

In the next step, the main analysis was done. First, the data was filtered with a high-pass filter. A Butterworth filter with a cut-off frequency of 0.5 Hz, second-order, and a padding length of 150 samples. The filter was chosen to detrend the signal and is assuming that the heart rate is lower than 120 BPM. The filter was run twice, once from the front and then from back to avoid any shifting. The absolute value

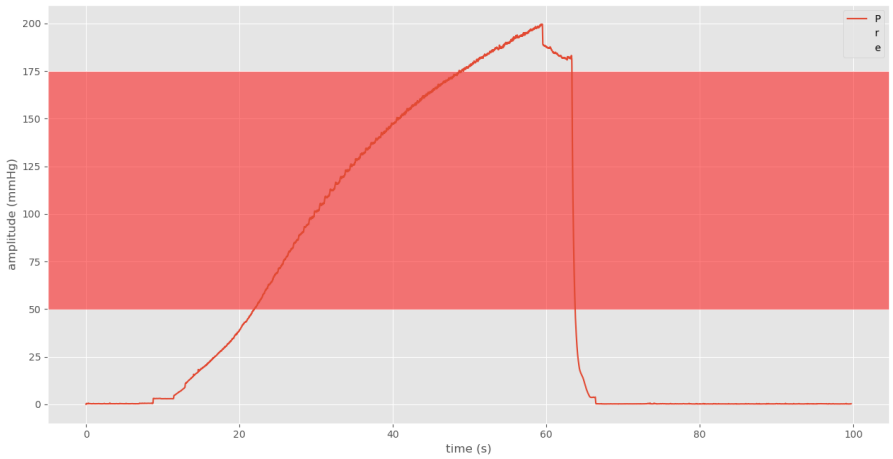

Figure 28: Selecting the region of interest after LP filtered data

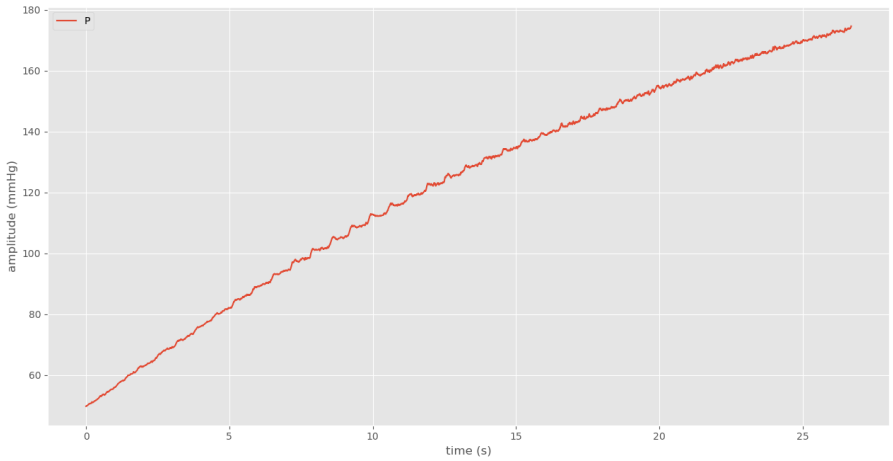

Figure 29: The selected region of interest

of the signal was counted so we wouldn't lose the information of negative values and the Hilbert transformation was applied to get the envelope. In this step, we expected a similar result as if we were acquiring the envelope in MATLAB but the envelope wasn't smooth enough due to the short length of the signal, thus our envelope had still many peaks. Therefore we counted the rolling mean of the envelope so that it would resemble the expected envelope. From this new envelope, we found the peak which had the same position as MAP and through a ratio of 0.74 of MAP value in the envelope for diastole and 0.7 of MAP value in the envelope for systole (The ratios were based of [47] and adjusted to the measured data), we found the position of the systolic and diastolic pressures. The filtered data with its old and new envelope and the positions of the acquired pressures is shown in figure 30.

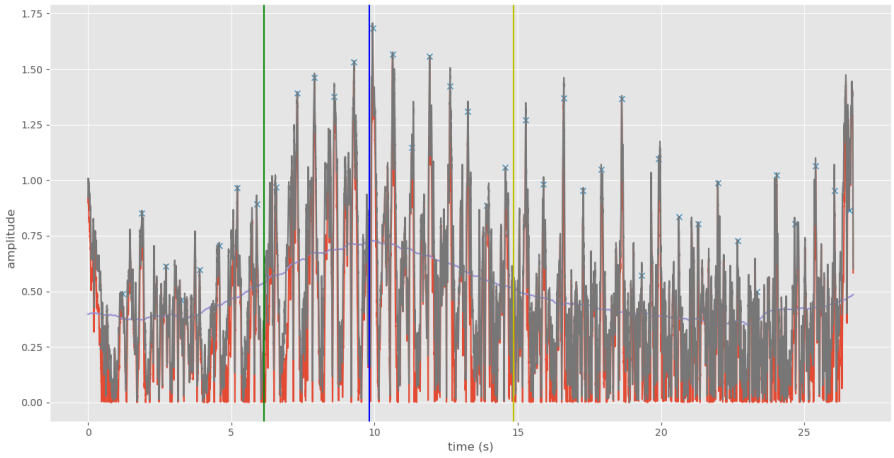

Figure 30: HP filtered data (red), envelope from the Hilbert transformation (grey), adjusted rolling mean of envelope (violet), peaks (blue crosses), MAP (Blue line), DIA (green line), SYS (yellow line)

In the last step, we plotted the region of interest with the positions of MAP and diastolic and systolic pressure (figure 31) and the script showed in the command line the values and heartrate counted from the peaks in the HP filtered data.

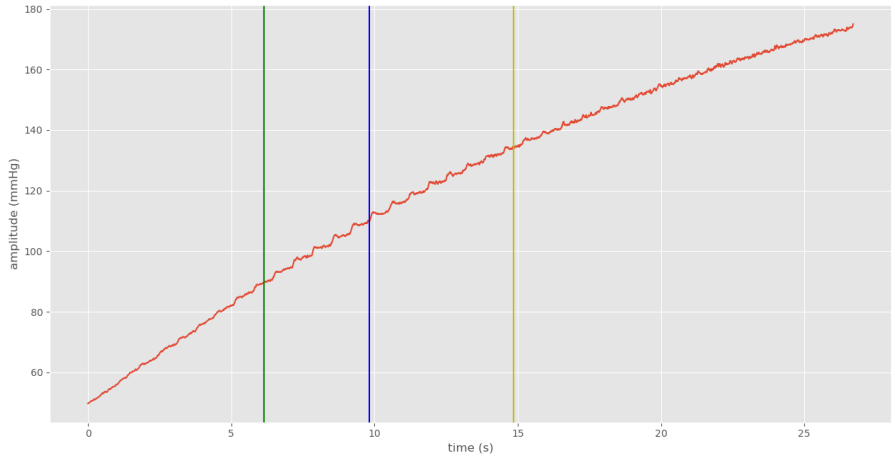

Figure 31: MAP (Blue line), DIA (green line) and SYS (yellow line) in the region of interest

4.5.4 PWV analysis script

In the PWV analysis, we started again with the loading of the data similarly to the blood pressure analysis. We plotted the data and used again a span selector, this time horizontal, for the user to choose a time frame where the closing valve was closed (the descending areas with pulsation) (figure 32). The selected region is shown in figure 33.

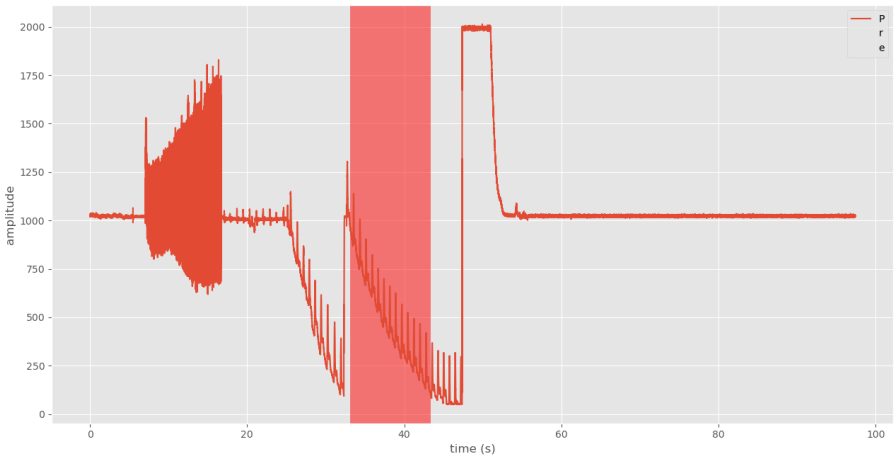

Figure 32: Selection of the region of interest from loaded data

The next step was to use a HP filter (figure 34). Again a Butterworth filter with a cut-off frequency of 0.7 Hz, second-order and a padding length of 150 samples. The cutoff frequency has been chosen to detrend the data, here we had to compromise since lower frequency couldn't fully detrend the data and the used frequency could intervene with the heart rate. Filter was run again from both sides to avoid any shifting.

Further, we filtered the data again with an LP filter (figure (35)) with a cut-off frequency of 20 Hz, an order of 101 and a "Hamming" window. The frequency has again been chosen from the spectrum magnitude of the signal, this time we wanted to smoothen the pressure pulse waves and get rid of as much of high frequency as possible.

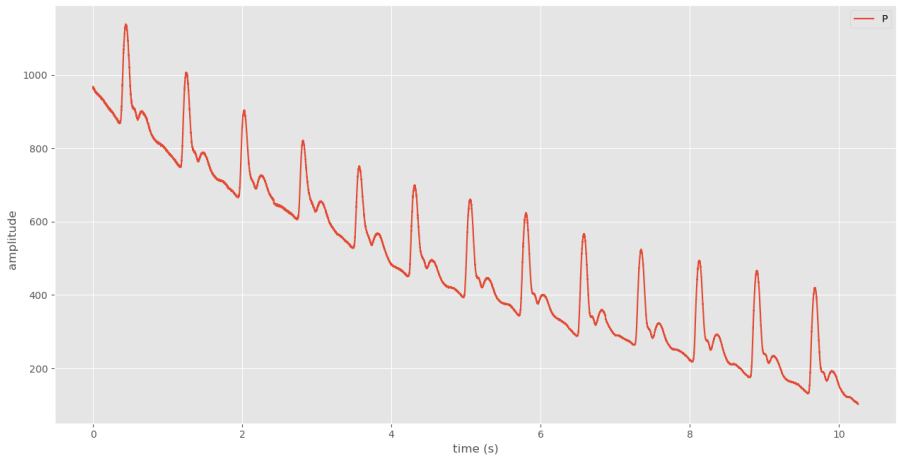

Figure 33: The region of interest

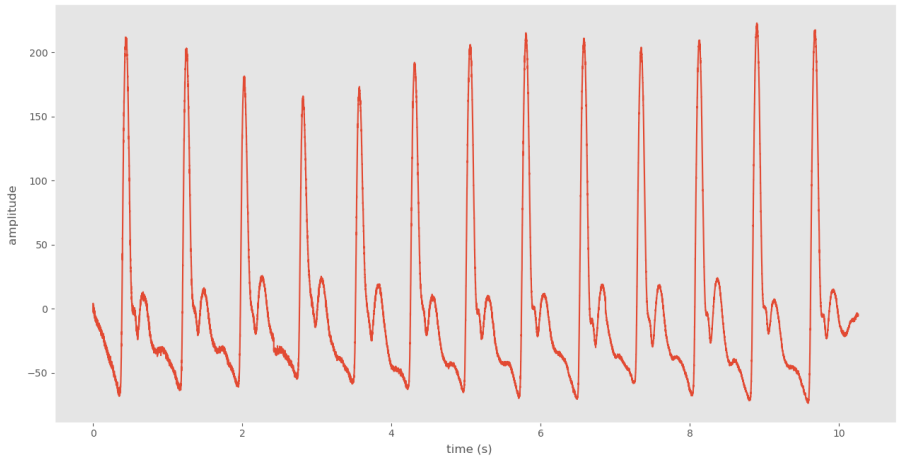

Figure 34: The HP filtered region of interest

In the next step, we normalized the y-axis values between 0 and 1 and found the peaks of the signal. In figure 36) the peaks and minima are shown. From the peaks, we counted the mean distance of the peaks.

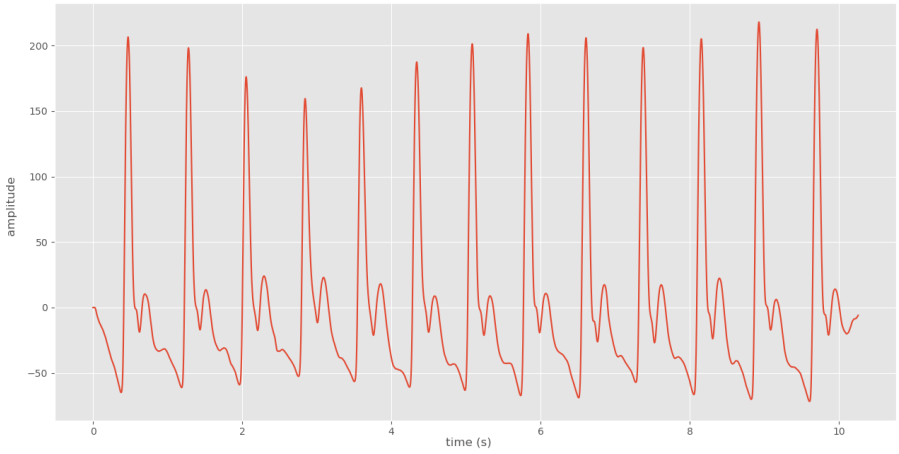

Figure 35: The LP filtered region of interest

Next, the Console asked the user to input the distance between the aorta and pubis, and saved the double of this distance, since the wave travels the distance twice.

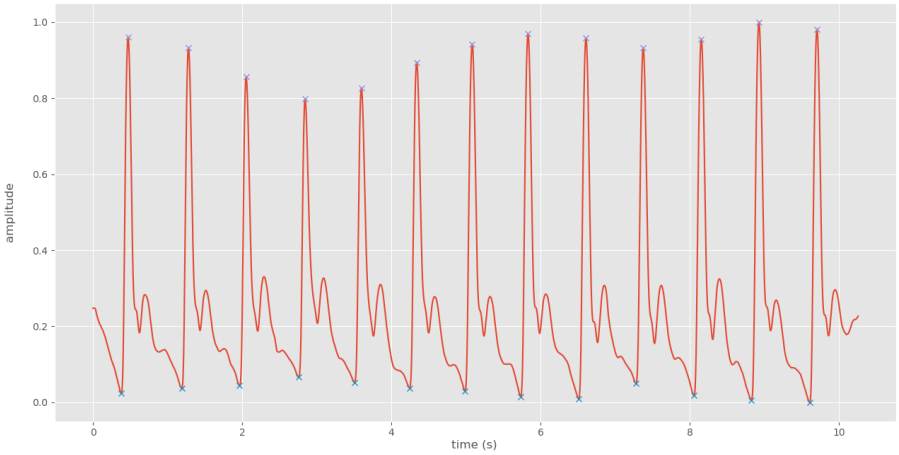

Figure 36: Peaks and minima in the normalised region of interest

Further, the main analysis began. The data was cut into segments by 0.2 average distance before a peak and 0.8 average distance after a peak. Afterwards, the second derivative was calculated and filtered by an LP filter with a cut-off frequency of 30 Hz to show the significant inflexion points and get rid off high-frequency noise. The local maxima and minima were counted from the first derivative of the signal. Then, a function found the most significant inflexion point between the peak and the minimum expected PWV. Afterwards, the wave was plotted with all these points and with the second derivative. For the manual selection, an area of expected PWV values was shown. In the manual selection, the user had to choose the area between the peak and the inflexion point, with the help of all the previously mentioned markers. One of the waves is shown in figure 37 After running through all the selected waves the PWV was counted from the selected and the automatically acquired delays, mean value and median were counted for both PWVs. The heart rate was counted from the peaks. Finally, all the results were shown in the console.

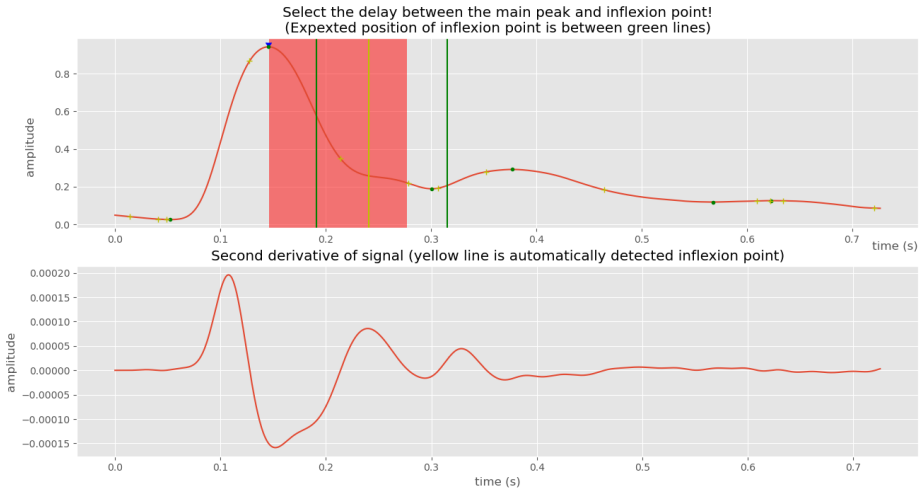

Figure 37: Analysis of a single waveform, top: red - the waveform, green lines - area of expected inflexion point, yellow line - the automatically detected inflexion point, blue triangle - peak, yellow crosses - inflexion points, green dots - local extrema, red area - selected PWV delay; bottom: second derivative of the signal

5 Validation measurement

To validate the proper function of the system we assessed a validation measurement. The voluntary participants were six students aged between 20 to 24 years. Two of the participants were female and four male. Three of the participants had a cardiovascular condition. The conditions were Arrhythmia with extrasystoles, chronic high blood pressure and chronic low blood pressure. A validation measurement of multiple age categories and a larger sample of healthy individuals would result in a more credible validation. But the conditions in the time of the measurement wouldn't allow us to assess a measurement on a larger scale.

For comparison to our results, we decided to use OMRON HEM-907 digital blood pressure monitor [48] for blood pressure measurement and heart rate measurement. A system using the same principle of suprasystolic pressure pulsations for assessing PWV [49]. The OMRON blood HEM-907 is also using the oscillometric method of blood pressure measurement, it is done during the deflation of the cuff which is at a speed of 2 mmHg/s The system had a pneumatic part that was controlled via BlueTooth through a computer. The data was captured with Biopac Student lab software through a BIOPAC system [50]. The data captured by the BIOPAC system was later evaluated through a program written in the Matlab programming language [23]. The validation of that system was done with the SphygmoCor system [49]. The measurements had to be done in succession with a small delay as possible, otherwise, the data wouldn't be comparable.

Figure 38: OMRON HEM-907 digital blood pressure monitor from steps one and three

5.1 Measurement protocol

The participant is suggested to not take any substances influencing the cardiovascular system before the measurement.

The first step, the blood pressure and heart rate of the participant are measured with the Omron blood pressure monitor. The participant is asked to put the cuff on his left arm. The measurement is done automatically by the device by pressing the "Start" button. The participant is asked to remain calm and not talk during the measurement. The values are noted.

The second step, the participant is measured with our designed system. Blood pressure is assessed. The participant is asked to put the cuff of our system on his left arm. He is asked to remain calm and not talk when told by the operator. The operator starts the capturing script and runs the automatic inflation in our system, the participant is told to remain calm. After reaching a level of 200 mmHg the cuff is deflated and the data is stored. The evaluation is run after all the measurements.

Figure 39: Our designed system from step two and three

The third step, the participant is measured with our designed system and OMRON blood pressure monitor. The PWV and heart rate are assessed. The participant is still seated with the cuff on his left arm and is asked to remain calm and not talk when told by the operator. Additionally, he is asked to put on the cuff of the OMRON

blood pressure monitor on his right arm. The operator starts the capturing script and manually inflates the cuff to the suprasystolic pressure level and simultaneously starts the OMRON blood pressure monitor. The suprasystolic levels are obtained from step one by adding 30 mmHg to the systolic blood pressure. After reaching the suprasystolic pressure, the operator waits for the pressure to stabilise, asks the participant to remain calm and closes the closing valve. The data is being captured for around 10 s. The operator deflates the cuff and the data is stored. The heart rate value from OMRON monitor is noted. The evaluation of data is run after the measurements.

The fourth step, the participant is measured with the system using suprasytolic pressure oscillation with capturing through a BIOPAC system. The PWV is assessed. The participant is asked to put the cuff on his left arm and is asked to remain calm and not talk when told by the operator. The operator sets and runs the automatic inflation. When inflated the operator levels the system and asks the participant to remain calm and. The data is being captured for around 10 s. The operator deflates the cuff. The data is stored, The evaluation is run after the measurements.

Figure 40: The PWV measuring system using BIOPAC from step four

Fifth step, data about the participants are surveyed. The data is height, weight and the distance between Aorta and Pubis. All the data is anonymous.

The measurements from the second to the fourth step are evaluated. The measurements of the second and third step are evaluated through scripts run in Python programming language run on a PC. The measurement of the fourth step is evaluated through scripts run in Matlab programming language run on a PC. Blood pressure, PWV and HR are being assessed The values are noted.

6 Results

The captured data was stored and evaluated on a PC (Personal computer). The evaluation was done through the scripts shown in the section "Technical documentation" subsection "Software". During the blood pressure analysis, we noticed that the data of three participants didn't show any oscillometric pulsation therefore we couldn't compute the blood pressure levels. The data of one participant was badly recorded on the BIOPAC system and couldn't be evaluated either.

6.1 Blood pressure

In the following table 6, there is a comparison of the blood pressures measured by the OMRON digital blood pressure monitor and the pressures we acquired through our algorithm.

Table 6: Blood pressure measurement

Participant:	Gender:	OMRON SYS/DIA (mmHg)	Our System SYS/DIA (mmHg)	MAP (mmHg)
2	male	124/75	128/79	112
3	female	119/76	135/86	102
6	male	136/95	142/85	110

It was difficult to evaluate the measured values since the blood pressure levels can change in a very short time due to the current state of the participant during the measurement. We could see that our values were higher than the values measured with OMRON, although the last participant was suffering from chronic high blood pressure. The values could be subjected to a systemic error, that could be removed since the oscillations we saw resembled the oscillometric method oscillations. The other three participants had lower blood pressures than these participants, to begin with. This may have caused that the oscillation couldn't be detected. A suggestion would be to inflate the cuff even slower at a rate of 3 mmHg/s (the rate used was 7 mmHg/s).

6.2 Pulse wave velocity

The results of PWV measurement are shown in table 7. The values were required through scripts in Matlab and Python. It is important to notice that the data was measured on different systems at different times and the data evaluated by Matlab scripts came from the system with BIOPAC and the data evaluated by Python came from our system, thus the script could also be run on our system.

Table 7: PWV measurement

Participant:	Gender:	Distance aorta-pubis (cm)	PWV BIOPAC and Matlab (m/s)	PWV Python Automatic (m/s)	PWV Python Manual (m/s)
1	female	27	3.46	5.54 ± 0.92	3.45 ± 0.42
2	male	48	9.60	5.56 ± 0.26	8.80 ± 0.52
3	female	31	5.44	5.81 ± 1.11	5.44 ± 0.58
4	male	36	4.80	5.51 ± 1.00	4.97 ± 0.63
5	male	33	4.61	4.63 ± 0.52	4.70 ± 0.54
6	male	34	NA	6.95 ± 0.48	5.68 ± 0.55

We can see that our manually acquired PWV resembles the values acquired by the BIOPAC system. The automatic system had issues to recognize the proper inflexion points. This is due to the large variability in the pulse waveform forms. Our automatic algorithm seems to have worked with the waveform type of participant 5. The results mainly for the manual algorithm compared to the other system, which has been validated [49], seem valid and the system should be capable of proper pulse-wave analysis and determination of PWV. The computation of the uncertainties is explained in the next section.

6.3 Heart rate

The last measured hemodynamic parameter was the heart rate. During the measurement, we followed the "The British Hypertension Society (BHS) validation protocol" [51]. The measured values are shown in table 6.3.

Table 8: Heart rate measurement

Participant:	Heart rate * OMRON (BPM)	Heart rate** OMRON (BPM)	Heart rate** Python (BPM)
1	66	61	62
2	68	67	67
3	94	91	92
4	69	70	70
5	75	80	80
6	93	80	80

* Independent measurement, ** Simultaneous measurement;

We can see that our values were almost the same as the values measured with Omron blood pressure monitor during the simultaneous measurement. The BHS validation allows for a difference of 2 BPM which we achieved, therefore the heart rate measurement was valid.

6.4 Measurement uncertainty

Every measurement is subject to an uncertainty[52]. Uncertainty quantifies the doubt about the measurement result, therefore the results of the measurements should be given with an interval of measurement uncertainty. It comes from the measuring devices, the measured subject, the process of measurement and the environment. The effects can be either random or systemic. The random effect adds a random uncertainty to each measurement whereas the systemic effects influence each measurement in the same way and can be removed by adjusting the measurement or finding a different approach. To estimate the uncertainty, no matter if caused by a random or systemic effect, we can use two evaluations. The "type A" evaluation uses statistics of multiple readings to determine the uncertainty. The "type B" evaluation uses nonstatistical methods, like the scale and distinction of the measuring instruments, the error of

reading by the operator, before acquired data and calibration.[52]

The calculation of the "type A" uncertainty goes as followed. From the readings, we count the arithmetic mean (equation 15). Then we calculate the standard deviation (equation 16). Finally putting all together, the "type A" uncertainty is defined by equation 17 [52].

$$\bar{x} = \frac{1}{N}\sum_{k=1}^{N} x_i \tag{15}$$

$$s = \sqrt{\frac{1}{N-1}\sum_{k=1}^{N}(x_i - \bar{x})^2} \tag{16}$$

$$u_A = \frac{s}{\sqrt{N}} = \sqrt{\frac{\sum_{k=1}^{N}(x_i - \bar{x})^2}{N \cdot (N-1)}} \tag{17}$$

Where x is the single readings, $\bar{x}$ is the arithmetic mean, N is the number of readings and s is the standard deviation.

In our case, the "type B" uncertainty is calculated from the distinctive capability of the time measurement and the error caused by the operator while reading the distance between aorta and pubis. For the distinction capabilities of the device we use the equation 18 and for the operator caused error we use the equation 19 [53].

$$u_B = \frac{\Delta}{\sqrt{12}} \tag{18}$$

$$u_B = \frac{\Delta}{\sqrt{3}} \tag{19}$$

Where Δ is the error or distinction capability.

In our case, the time distinction was given by the ADC capabilities which were at 2 kHz 500 μs and the error of distance reading that was 3 cm.

To get the total uncertainty we need to take into account all the uncertainties with the calculation (equation 20) [53].

$$U_C(X) = 2 \cdot \sqrt{(\frac{\delta X}{\delta X'})^2 \cdot u^2(X') + (\frac{\delta X}{\delta K})^2 \cdot u^2(K)} \tag{20}$$

For the calculation of PWV, we used the equation 21. Substituting into the previous equation we get the equation 22.

$$PWV = \frac{2d}{t} \qquad [\frac{\mathrm{m}}{\mathrm{s}}] \tag{21}$$

Where d is the distance between aorta and pubis and t is the delay of the reflected wave.

$$U_C(PWV) = 2 \cdot \sqrt{(\frac{\delta PWV}{\delta d})^2 \cdot u_C^2(d) + (\frac{\delta PWV}{\delta t})^2 \cdot u_C^2(t)} \qquad [\frac{\mathrm{m}}{\mathrm{s}}] \tag{22}$$

Where $u_C(d)$ is the total uncertainty of distance , given in our case by the "type B" uncertainty and $u_C(t)$ is the total uncertainty of time, given by the "type A" and "type B" uncertainties combined (equation 23) [53].

$$u_C(t) = \sqrt{u_A^2(t) + u_B^2(t)} \qquad [\mathrm{s}] \tag{23}$$

Finally, the total uncertainty of our PWV measurement is shown in equation 24

$$U_C(PWV) = 2 \cdot \sqrt{(\frac{2}{t})^2 \cdot (\frac{0.03}{\sqrt{3}})^2 + (2d\frac{-1}{t^2})^2 \cdot (\frac{s_t^2}{N_t} + (\frac{\frac{1}{2000}}{\sqrt{12}})^2)} \qquad [\frac{\mathrm{m}}{\mathrm{s}}] \tag{24}$$

Where d is the distance between aorta and pubis, t is the delay of the reflected wave,N_t is the number of readings of delay and s_t is the standard deviation of the delay.

7 Conclusion

This master's thesis aimed to assemble and test a system for non-invasive measurement of hemodynamic parameters with an inflatable cuff over the Brachial artery. Our system used two principles to assess the hemodynamic parameter. The first principle was based on the oscillometric method used for blood pressure measurement, we have tried to use this method during the slow inflation of the cuff to get the blood pressure values. The second principle used was inflating the cuff to a suprasystolic pressure level and through a differential sensor capturing the pulse waveforms. The waveforms were then further analysed to assess pulse-wave velocity and heart rate. All using the open-sourced platforms of Raspberry pi for hardware and Python programming language for software.

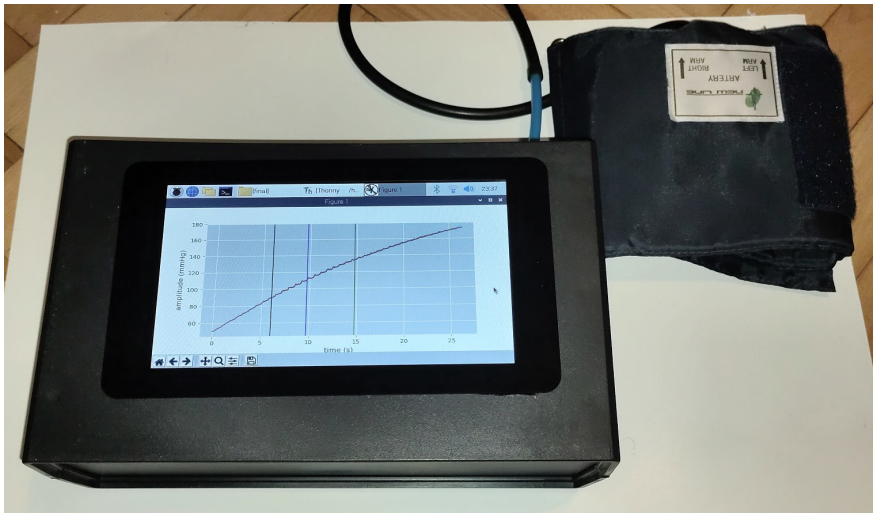

Figure 41: The final proposed system

In the first part, we researched hemodynamic parameters that could be measured non-invasively with our system. Although the Analysis of the pulse waveform offers many parameters and indexes, we decided to measure the blood pressure, namely the mean arterial pressure, the diastolic blood pressure and the systolic blood pressure, further the pulse wave velocity and the heart rate. There are more options to assess other parameters since our system captures a continuous pulse-wave signal.

In the next part, we researched the tools we were using. The raspberry pi microcomputer had substantial computational power to run all our programs and control all the

needed components and enough inputs and outputs to connect. All the needed software and controlling scripts could be written in The Python programming language. The support for Python on the Raspberry pi was helpful during the development of the software.

The technical documentation contains all the used parts in all the different components. The pneumatic component was controlled through the raspberry pi and allowed for transduction of the pressure pulse-wave to our sensors. The values were read by an analogue to digital converter and send to the raspberry pi. Further, we used a touchscreen for displaying information and user input and a battery pack to allow the device to be portable. The process of all the measured hemodynamic parameters was also described in the documentation.

The proposed system was tested on six voluntary participants in the age between 20 and 24 years. The measured data were compared to systems running on similar principles and measuring the hemodynamic parameters of interest. The validation of the blood pressure measurement wasn't sufficient due to the system not being able to pick up low-pressure oscillation and the small number measured values. The pulse-wave velocity analysis, namely the proposed manual solution proved to be working and therefore the system could be used for further pulse waveform analysis. The heart rate analysis worked as well since it was based on the pulse-wave velocity analysis.

Many people could benefit from a portable device that would measure noninvasively hemodynamic parameters and assess an examination on the risk of cardiovascular diseases. The device in its current form can measure the pulse waveform and assess the pulse-wave velocity and heart rate. with some additional algorithms, it could further analyse the pressure pulse wave and require the needed parameters for this examination.

References

1. *Cardiovascular diseases statistics - Statistics Explained*. 2019. Available also from: https://ec.europa.eu/eurostat/statistics-explained/index.php/Cardiovascular_diseases_statistics.
2. *Cardiovascular diseases (CVDs)*. 2017. Available also from: https://www.who.int/news-room/fact-sheets/detail/cardiovascular-diseases-(cvds).
3. MAGDER, S. The meaning of blood pressure. *Critical Care*. 2018, vol. 22, no. 1, pp. 257. ISSN 1364-8535. Available from DOI: 10.1186/s13054-018-2171-1.
4. SALVI, Paolo. *Pulse waves: how vascular hemodynamics affects blood pressure*. Springer, 2012. ISBN 978-88-470-2438-0.
5. GOONASEKERA, C. D. A.; DILLON, M. J. Measurement and interpretation of blood pressure. *Archives of Disease in Childhood*. 2000, vol. 82, no. 3, pp. 261–265. ISSN 0003-9888, 1468-2044. ISSN 0003-9888, 1468-2044. Available from DOI: 10.1136/adc.82.3.261.
6. PAUL, Muntner et al. Measurement of Blood Pressure in Humans: A Scientific Statement From the American Heart Association. *Hypertension*. 2019, vol. 73, no. 5, pp. e35–e66. Available from DOI: 10.1161/HYP.0000000000000087.
7. ORTOVÁ, Bc Jana. DESIGN AND REALIZATION OF A DEVICE FOR OSCILLOMETRIC PULSATION SENSING, pp. 76.
8. D., Sesso Howard; J., Stampfer Meir; BERNARD, Rosner; H., Hennekens Charles; MICHAEL, Gaziano J.; E., Manson JoAnn; J., Glynn Robert. Systolic and Diastolic Blood Pressure, Pulse Pressure, and Mean Arterial Pressure as Predictors of Cardiovascular Disease Risk in Men. *Hypertension*. 2000, vol. 36, no. 5, pp. 801–807. Available from DOI: 10.1161/01.HYP.36.5.801.
9. Arterial Pressure Waveforms. In: *Basic Physiology for Anaesthetists*. 2nd ed. Cambridge University Press, 2019, pp. 155–157. ISBN 978-1-108-46399-7. Available from DOI: 10.1017/9781108565011.038.
10. *Understanding Blood Pressure Readings*. Available also from: https://www.heart.org/en/health-topics/high-blood-pressure/understanding-blood-pressure-readings.

11. JACQUES, Blacher; ROLAND, Asmar; SALIHA, Djane; M., London Gérard; E., Safar Michel. Aortic Pulse Wave Velocity as a Marker of Cardiovascular Risk in Hypertensive Patients. *Hypertension*. 1999, vol. 33, no. 5, pp. 1111–1117. Available from DOI: 10.1161/01.HYP.33.5.1111.

12. COSTELLO, Benedict T.; SCHULTZ, Martin G.; BLACK, J. Andrew; SHARMAN, James E. Evaluation of a brachial cuff and suprasystolic waveform algorithm method to noninvasively derive central blood pressure. *American Journal of Hypertension*. 2015, vol. 28, no. 4, pp. 480–486. ISSN 1941-7225. Available from DOI: 10.1093/ajh/hpu163.

13. SANGKUM, Lisa; LIU, Geoffrey L.; YU, Ling; YAN, Hong; KAYE, Alan D.; LIU, Henry. Minimally invasive or noninvasive cardiac output measurement: an update. *Journal of Anesthesia*. 2016, vol. 30, no. 3, pp. 461–480. ISSN 1438-8359. Available from DOI: 10.1007/s00540-016-2154-9.

14. PITT, Marjorie; MARSHALL, Paul; DIESCH, Jonathan; HAINSWORTH, Roger. Cardiac output by Portapres (R). *Clinical science (London, England: 1979)*. 2004, vol. 106, pp. 407–12. Available from DOI: 10.1042/CS20030279.

15. WALDRON, Mark; DAVID PATTERSON, Stephen; JEFFRIES, Owen. Inter-Day Reliability of Finapres ® Cardiovascular Measurements During Rest and Exercise. *Sports Medicine International Open*. 2017, vol. 2, no. 1, pp. E9–E15. ISSN 2367-1890. Available from DOI: 10.1055/s-0043-122081.

16. NICKSON, Dr Chris. *PiCCO • LITFL • CCC Equipment*. 2019. Available also from: https://litfl.com/picco/.

17. CHEUNG, Yiu-fai. CHAPTER 6 - Systemic Circulation. In: *Paediatric Cardiology (Third Edition)*. Ed. by ANDERSON, Robert H.; BAKER, Edward J.; PENNY, Daniel J.; REDINGTON, Andrew N.; RIGBY, Michael L.; WERNOVSKY, Gil; PRICE, Gemma. Churchill Livingstone, 2010, pp. 91–116. ISBN 978-0-7020-3064-2. Available from DOI: 10.1016/B978-0-7020-3064-2.00006-0.

18. QUINN, Ursula; TOMLINSON, Laurie A; COCKCROFT, John R. Arterial stiffness. *JRSM Cardiovascular Disease*. 2012, vol. 1, no. 6. ISSN 2048-0040. Available from DOI: 10.1258/cvd.2012.012024.

19. WESTENBERG, Jos JM; POELGEEST, Eveline P van; STEENDIJK, Paul; GROTENHUIS, Heynric B; JUKEMA, JW; ROOS, Albert de. Bramwell-Hill modeling for local aortic pulse wave velocity estimation: a validation study with velocity-encoded cardiovascular magnetic resonance and invasive pressure assess-

ment. *Journal of Cardiovascular Magnetic Resonance*. 2012, vol. 14, no. 1, pp. 2. ISSN 1097-6647. Available from DOI: 10.1186/1532-429X-14-2.

20. HUSMANN, Marc; JACOMELLA, Vincenzo; THALHAMMER, Christoph; AMANN-VESTI, Beatrice. Markers of arterial stiffness in peripheral arterial disease. *VASA. Zeitschrift fur Gefasskrankheiten*. 2015, vol. 44, pp. 341–348. Available from DOI: 10.1024/0301-1526/a000452.

21. BALTGAILE, Galina. Arterial wall dynamics. *Perspectives in Medicine*. 2012, vol. 1, no. 1, pp. 146–151. ISSN 2211-968X. Available from DOI: 10.1016/j.permed.2012.02.049.

22. MCVEIGH, Gary E.; BANK, Alan J.; COHN, Jay N. Arterial Compliance. In: *Cardiovascular Medicine*. Ed. by WILLERSON, James T.; WELLENS, Hein J. J.; COHN, Jay N.; HOLMES, David R. Springer, 2007, pp. 1811–1831. ISBN 978-1-84628-715-2. Available from DOI: 10.1007/978-1-84628-715-2_88.

23. MATERA, Lukáš. Analýza slabých tlakových pulzací při suprasystolickém tlaku. 2017. Available also from: https://dspace.cvut.cz/handle/10467/68535.

24. REFAAT, Alaa; ABDOU, Mohamed; ISMAEL, Ali; ALHELALI, Ihab. Aortic stiffness and microalbuminuria in patients with chronic obstructive pulmonary disease. 2015, vol. 21. Available from DOI: 10.1016/j.ejcdt.2015.03.008.

25. F., Mitchell Gary. Arterial Stiffness and Hypertension. *Hypertension*. 2014, vol. 64, no. 2, pp. 210–214. Available from DOI: 10.1161/HYPERTENSIONAHA.114.03449.

26. FLEENOR, Bradley S.; BERRONES, Adam J. *Arterial Stiffness: Implications and Interventions*. Springer, 2015. ISBN 978-3-319-24844-8. Google-Books-ID: 3dkLCwAAQBAJ.

27. BARRACLOUGH, Jennifer Y.; GARDEN, Frances L.; TOELLE, Brett; O'MEAGHER, Shamus; MARKS, Guy B.; COWELL, Christopher T.; CELERMAJER, David S.; AYER, Julian G. Sex differences in aortic augmentation index in adolescents. *Journal of Hypertension*. 2017, vol. 35, no. 10, pp. 2016–2024. Available from DOI: 10.1097/HJH.0000000000001425.

28. SIEVI, Noriane; FRANZEN, Daniel; KOHLER, Malcolm; CLARENBACH, Christian. Physical inactivity and arterial stiffness in COPD. *International journal of chronic obstructive pulmonary disease*. 2015, vol. 10, pp. 1891–1897. Available from DOI: 10.2147/COPD.S90943.

29. SALVI, Paolo. *Pulse Waves: How Vascular Hemodynamics Affects Blood Pressure*. Springer, 2016. ISBN 978-3-319-40501-8.

30. MIDDLETON, PM; RETTER, A; HENRY, JA. Pulse oximeter waveform analysis as a measure of circulatory status. *Critical Care*. 2001, vol. 5, no. Suppl 1, pp. P152. ISSN 1364-8535. Available from DOI: 10.1186/cc1219.

31. BENETOS, Athanase; THOMAS, Frédérique; JOLY, Laure; BLACHER, Jacques; PANNIER, Bruno; LABAT, Carlos; SALVI, Paolo; SMULYAN, Harold; SAFAR, Michel E. Pulse Pressure Amplification: A Mechanical Biomarker of Cardiovascular Risk. *Journal of the American College of Cardiology*. 2010, vol. 55, no. 10, pp. 1032–1037. ISSN 0735-1097, 1558-3597. ISSN 0735-1097, 1558-3597. Available from DOI: 10.1016/j.jacc.2009.09.061.

32. XIA, Jingjing; LIAO, Simon. Pulse wave analysis for cardiovascular disease diagnosis. *Digital Medicine*. 2018, vol. 4, pp. 35. Available from DOI: 10.4103/digm.digm_2_18.

33. CEO, Craig Cooper-CardieX. *What is SphygmoCor?* 2019. Available also from: https://cardiex.com/what-is-sphygmocor/.

34. LOWE, Andrew; HARRISON, W; EL-AKLOUK, E; RUYGROK, P; AL-JUMAILY, Ahmed. Non-invasive model-based estimation of aortic pulse pressure using suprasystolic brachial pressure waveforms. *Journal of biomechanics*. 2009, vol. 42, pp. 2111–5. Available from DOI: 10.1016/j.jbiomech.2009.05.029.

35. Raspberry Pi, 2020. Available also from: https://github.com/raspberrypi/documentation.

36. *pi3-block-diagram-rev4.png (1259900)*. Available also from: https://www.element14.com/community/servlet/JiveServlet/downloadImage/38-24733-365232/1259-900/pi3-block-diagram-rev4.png.

37. *Debian*. Available also from: https://www.debian.org/index.cs.html.

38. *LXDE.org*. Available also from: https://wiki.lxde.org/en/Main_Page.

39. *Openbox*. Available also from: http://openbox.org/wiki/Main_Page.

40. *Raspberry Pi*. Available also from: https://www.raspberrypi.org/.

41. *DietPi*. Available also from: https://dietpi.com/.

42. *Python.org*. Available also from: https://www.python.org/.

43. COMPANY, The Qt. *Qt — Cross-platform software development for embedded desktop*. Available also from: https://www.qt.io.

44. *Kivy.org*. Available also from: http://kivy.org/.

45. MARIATOS, E.P.; MERAKOS, P.; BIRBAS, Michael; BIRBAS, Alexios. Hardware programming using C++. *Microprocessing and Microprogramming*. 1994, vol. 40, pp. 817–820. Available from DOI: 10.1016/0165-6074(94)90047-7.

46. *MATLAB*. Available also from: https://www.mathworks.com/products/matlab.html.

47. LIU, Jiankun; HAHN, Jin-Oh; MUKKAMALA, Ramakrishna. Error Mechanisms of the Oscillometric Fixed-Ratio Blood Pressure Measurement Method. *Annals of biomedical engineering*. 2012, vol. 41. Available from DOI: 10.1007/s10439-012-0700-7.

48. *HEM-907 - Blood Pressure Monitor - Omron Healthcare Asia Pacific*. Available also from: https://www.omronhealthcare-ap.com/ap/product/93-hem-907/1.

49. FABIAN, Vratislav; MATERA, Lukas; BAYEROVA, Kristyna; HAVLIK, Jan; KREMEN, Vaclav; PUDIL, Jan; SAJGALIK, Pavol; ZEMANEK, David. Noninvasive Assessment of Aortic Pulse Wave Velocity by the Brachial Occlusion-Cuff Technique: Comparative Study. *Sensors*. 2019, vol. 19, no. 1616, pp. 3467. Available from DOI: 10.3390/s19163467.

50. *Practical Lab Kit for Remote Learning — BSL-HOME — Education — BIOPAC*. Available also from: https://www.biopac.com/product/bsl-home/.

51. O'BRIEN, Eoin; SWIET, Michael de; BLANDG, Martin; ATKINS, Neil. The British Hypertension society protocol for the k.1 evaluation of blood preskure measuring devices, pp. 20.

52. BELL, Stephanie. Measurement Good Practice Guide No. 11 (Issue 2), pp. 41.

53. ČERVENKA, Milan. Zpracování fyzikálních měření. Studijní text pro fyzikální praktikum. 2013.

Appendices

Contents:

Appendix A

Contents of the CD:

- Blood_pressure
  - contro_GUI.py
  - my.kv
  - pressure.py
  - readADC.c
- PWV
  - contro_GUI.py
  - my.kv
  - PWV.py
  - readADC.c
- Continuous_read
  - contro_GUI.py
  - my.kv
  - read.py
  - spidev3202.py